
Electronic Thesis and Dissertation Repository

9-21-2022 1:30 PM

The Biosynthesis of Non-protein Sulfur Amino Acid in Developing Seeds of Common Bean

Zixuan Lu, *The University of Western Ontario*

Supervisor: Marsolais, Frédéric, *The University of Western Ontario*

Co-Supervisor: Bernards, Mark, *The University of Western Ontario*

A thesis submitted in partial fulfillment of the requirements for the Master of Science degree in Biology

© Zixuan Lu 2022

Follow this and additional works at: <https://ir.lib.uwo.ca/etd>



Part of the [Agricultural Science Commons](#), and the [Plant Biology Commons](#)

Recommended Citation

Lu, Zixuan, "The Biosynthesis of Non-protein Sulfur Amino Acid in Developing Seeds of Common Bean" (2022). *Electronic Thesis and Dissertation Repository*. 8963.

<https://ir.lib.uwo.ca/etd/8963>

This Dissertation/Thesis is brought to you for free and open access by Scholarship@Western. It has been accepted for inclusion in Electronic Thesis and Dissertation Repository by an authorized administrator of Scholarship@Western. For more information, please contact wlsadmin@uwo.ca.

Abstract

The protein quality of common bean (*Phaseolus vulgaris*) is associated with the level of dietary essential sulphur amino acids – methionine and cysteine. Extra sulphur that cannot be stored in the protein pool accumulates as the non-protein amino acid *S*-methylcysteine (*S*-methylCys) and its dipeptide γ -glutamyl-*S*-methylcysteine (γ -Glu-*S*-methylCys). Previous studies have indicated that *S*-methylhomogluthathione (*S*-methylhGSH) is present in the developing seed of common bean. It is hypothesized that *S*-methylhGSH is the key intermediate in the biosynthetic pathway of the γ -Glu-*S*-methylCys that leads to the accumulation of this dipeptide. This project elucidated the unknown biochemical pathway of *S*-methylhGSH synthesis using ³⁴S labeled methionine and ¹³C labeled sodium thiomethoxide in feeding experiments with developing seeds. The results suggest *S*-methylhGSH is synthesized by methylation of homogluthathione (hGSH). Biochemical assay with seed extract suggested γ -glutamyl transferase (GGT) is likely to catalyzing the reaction between hGSH and *S*-methylCys to produce γ -Glu-*S*-methylCys. Furthermore, benzoic acid was identified as the inhibitor for enzyme β -substituted alanine synthase 4;1 (BSAS4;1), which catalyzes the synthesis of *S*-methylCys. The findings delineate the biosynthetic pathways of the sulphur metabolome and provide potential approach to improve nutritional quality of common bean.

Keywords: *Phaseolus vulgaris*; sulphur amino acids; *S*-methylhomogluthathione; γ -glutamyl-*S*-methylcysteine; γ -glutamyl transferase; benzoic acid; common bean

Summary for Lay Audience

Common bean (*Phaseolus vulgaris*) is one of the most consumed legume crops in the world. This is especially true in developing countries. However, the protein quality in common bean is poor. This is due to the low level of essential sulphur amino acids, methionine and cysteine. Previous studies showed that instead of making methionine and cysteine, common beans make other sulphur containing compounds called non-protein sulphur amino acids. These non-protein sulphur amino acids are stored in common bean seeds. One way to improve protein quality in common bean seed would be to increase the amount of methionine and cysteine. This could be done by shifting sulphur away from non-protein sulphur amino acids and into methionine and cysteine. To be able to do this, we need to better understand the way non-protein sulphur amino acids are formed. Only then can we prevent them from being formed.

In my study, the biosynthesis of an important component in the formation of one non-protein sulphur amino acid was revealed. This new information provides clues to the identity of the enzyme involved in this pathway. Another enzyme, γ -glutamyl transferase (GGT), was shown to be involved in the biosynthesis a different non-protein sulphur amino acid. I also showed that GGT present in the seed of common bean accumulates in cell cytoplasm. This suggests a possible site of action for GGT. A third enzyme involved in non-protein sulphur amino acid, called BSAS4;1, was shown to be inhibited by the compound benzoic acid. This was true both in test tube reactions and in live bean seed cells. Altogether, my research findings could aid future efforts to improve the nutritional quality of common bean seeds, and contribute to the relief of malnutrition in the developing world.

Co-Authorship Statement

The candidate, Zixuan Lu, designed and performed the experiments, drafted the manuscript and analysed the data. Dr. Frédéric Marsolais provided the initial motivation for this research and strategic direction for the projects. Dr. Mariusz Jaskolski and his research team provided the crystal structure of BSAS4;1. Agnieszka Pajak contributed to HPLC measurements of different metabolites in enzyme assays. Dr. Justin Renaud contributed to seed sample analysis on the mass spectrometer and isotope incorporation data analysis. Revisions for improvement of the thesis were also provided by Dr. Frédéric Marsolais and Dr. Mark Bernards.

Acknowledgments

First and foremost, I would like to thank my supervisor Dr. Frédéric Marsolais for his guidance, consistent support and the belief he has shown in me. The passion he brings to plant research greatly inspired and motivated me to work diligently and efficiently over the past two years. He provided professional, knowledgeable, and patient guidance that allowed me to navigate the research and plan the experiments and learn immensely from the experience. I sincerely appreciate his inspirational leadership and am very grateful to have this opportunity to work on this project. I remain indebted to my co-supervisor, Dr. Mark Bernards, for his guidance, support and valuable comments to my proposal and thesis, also for inculcating a desire to give best in everything. The advisory committee has been a great scientific support through this journey, thank you Dr. Sangeeta Dhaubhadel and Dr. Susanne Kohalmi.

I am very lucky to have Aga Pajak as our lab technician, thank you for all the training and technical support, and for doing HPLC analysis for my samples. Working with you in the lab has been such a delight and everything I learned from you fostered me to be a better person. My sincere thanks to Dr. Justin Renaud for his collaboration on mass spectrometry analysis, patient guidance and valuable suggestions on sample preparation. I am also thankful to my present and former lab members, Dristy Zaman, Zhujun Qiu and Kaylee Versteegh for their assistance and memorable friendship. I would also like to thank staff and students at AAFC and Western University Biology who have helped and supported me through this journey.

Lastly, thank you to my family and friends for their encouragement and support throughout these past few years. Special thanks to Cynthia, Jasmine and James for their company and unconditional support. Every individual acknowledged here has contributed to and are recognized for the accomplishments of this research.

Table of Contents

Abstract.....	ii
Summary for Lay Audience.....	iii
Co-Authorship Statement	iv
Acknowledgments	v
Table of Contents	vi
List of Tables	x
List of Figures.....	xi
List of Appendices.....	xiii
List of Abbreviations	xiv
1 Introduction.....	1
1.1 Common bean	1
1.2 Seed storage proteins	1
1.3 Protein quality and sulphur metabolites.....	2
1.4 Sulphur metabolism in plants.....	4
1.5 Cysteine as a metabolic precursor.....	5
1.6 Biosynthesis of sulphur amino acid derivatives.....	6
1.7 Potential methods to improve protein quality in legumes	9
1.8 Research objectives.....	10
2 Materials and methods	12
2.1 Plant material and growth conditions	12
2.2 Determination of the mechanism of the biosynthesis of <i>S</i> -methylhGSH	12
2.2.1 Chemicals.....	12
2.2.2 Candidate genes for <i>S</i> -methylhomoglutathione synthesis	12

2.2.3	Cloning of candidate genes and recombinant protein purification	13
2.2.4	Seed protein extraction	14
2.2.5	Enzyme assays for <i>S</i> -methylhomoglutathione biosynthesis	14
2.2.5.1	Enzyme assay with GST protein.....	14
2.2.5.2	Enzyme assay with MT protein	14
2.2.6	Embryo culture and culture media.....	15
2.2.7	Isotope labelling treatment groups.....	15
2.2.8	Amino acid extraction and mass spectrometry analysis	16
2.3	The biosynthesis of γ -Glu- <i>S</i> -methylCys	17
2.3.1	Chemicals.....	17
2.3.2	Plant materials.....	17
2.3.3	Candidate genes for γ -glutamyl transferases.....	17
2.3.4	Cloning of GGT candidate genes for sub-cellular localization	17
2.3.5	Transient expression and confocal microscopy	18
2.3.6	Cloning for recombinant protein expression and purification	19
2.3.7	Soluble protein extraction from developing seeds	20
2.3.8	Assay of GGT activity	20
2.3.9	Enzyme assay	20
2.3.10	RT-PCR.....	21
2.4	Characterization of benzoic acid as an inhibitor.....	22
2.4.1	Chemicals.....	22
2.4.2	Recombinant protein purification and size-exclusion chromatography	22
2.4.3	Biochemical and kinetic assay	22
2.4.4	Embryo culture and culture media.....	23
2.4.5	Amino acid extraction and MS analysis	23
3	Results	24
3.1	Determination of the mechanism of the biosynthesis of <i>S</i> -methylhGSH	24

3.1.1	Tracking the fate of isotope labeled sodium thiomethoxide and methionine	24
3.1.2	Enzyme assay for <i>S</i> -methylhomoglutathione synthesis	30
3.1.2.1	Candidate genes for <i>S</i> -methylhomoglutathione synthesis	30
3.1.2.2	Recombinant protein purification and enzyme assays	33
3.2	Study of the biosynthesis of γ -Glu- <i>S</i> -methylCys	34
3.2.1	γ -Glutamyl transpeptidase candidate genes for γ -Glu- <i>S</i> -methylCys biosynthesis	34
3.2.2	Biochemical assay with γ -GPNA	35
3.2.3	Enzyme assay with seed extract	38
3.2.4	GGT protein purification	40
3.2.5	Transcripts expression of PvGGT1 and PvGGT4	41
3.2.6	Subcellular localization	44
3.3	Characterization of benzoic acid as an inhibitor of PvBSAS4;1	47
3.3.1	Biochemical assay for benzoic acid inhibition	47
3.3.1.1	Determination of optimal benzoic acid concentration for inhibition	47
3.3.1.2	Kinetic studies of benzoic acid	49
3.3.1.3	Inhibitory effect of other molecules similar to benzoic acid on PvBSAS4;1 ...	52
3.3.2	<i>In-vivo</i> assay with ¹³ C ¹⁵ N-labelled serine	54
3.3.2.1	<i>In-vivo</i> assay with benzoic acid	54
3.3.2.2	<i>In-vivo</i> assay with buthionine sulfoximine	56
4	Discussion	58
4.1	The biosynthesis of <i>S</i> -methylhomoglutathione	58
4.2	The biosynthesis of γ -Glu- <i>S</i> -methylCys	60
4.3	Characterization of benzoic acid as an inhibitor	62
5	Conclusion	66
5.1	Concluding remarks and future studies	66
	References	67

Appendices.....	74
Curriculum Vitae	79

List of Tables

Table 3.1: Molecular and genetic characteristics of methyltransferase (MT) and glutathione-S-transferase (GST) candidate genes.....	31
Table 3.2: Other methyltransferase genes tested in enzyme assays.....	32

List of Figures

Figure 1.1: The chemical structures of sulphur containing amino acids and <i>S</i> -derivatives in <i>Phaseolus. vulgaris</i>	3
.....	5
Figure 1.2 Simplified model of the sulphur assimilation to synthesize cysteine in plants.	5
Figure 1.3. Biosynthetic pathway of non-protein sulphur amino acids in the developing seed of common bean.	8
Figure 3.1: The study of non-protein sulphur amino acid biosynthetic pathway corresponding to sections in this thesis.	25
Figure 3.2a: Uptake and incorporation of ³⁴ S labeled methionine in developing seeds.	26
Figure 3.2b: Alternative scheme presenting ³⁴ S labeled methionine incorporated into <i>S</i> -containing metabolites in the non-protein sulphur amino acid biosynthetic pathway.	27
Figure 3.3a: Uptake and incorporation of ¹³ C labeled sodium thiomethoxide in developing seeds.	28
.....	28
Figure 3.3b: Alternative scheme presenting ¹³ C labeled sodium thiomethoxide incorporated into <i>S</i> -containing metabolites in the non-protein sulphur amino acid biosynthetic pathway.	29
Figure 3.4: Hydrophobic interaction chromatography of proteins from developing seeds.	36
Figure 3.5: GGT activity in different pooled fractions of seed proteins after hydrophobic interaction chromatography.	37
Figure 3.6: HPLC result of enzyme assay with homoglutathione and <i>S</i> -methylCys using seed extract as a source of GGT enzyme.	39

Figure 3.7: Assessment of expression level of different transcripts of <i>PvGGT1</i> and <i>PvGGT4</i> by RT-PCR.....	43
Figure 3.8: Subcellular localization of PvGGT4.2.	45
Figure 3.9: Subcellular localization of PvGGT1.2.	46
Figure 3.10: Inhibition of PvBSAS4;1 by benzoic acid.	48
Figure 3.11: Lineweaver-Burk plot for PvBSAS4;1 with a series of OAS and benzoic acid concentrations.	50
Figure 3.12: Dixon plot with a series of benzoic acid and OAS concentrations.	51
Figure 3.13: Inhibition of PvBSAS4;1 by salicylic acid.....	53
Figure 3.14: Percentage incorporation of labeled compounds in developing seeds following incubation with labeled serine in the presence and absence of benzoic acid.....	55
Figure 3.15: Percentage incorporation of labeled compounds in developing seeds following incubation with labeled serine in the presence and absence of BSO.....	57

List of Appendices

Appendix A: Expression profile of candidate genes in various plant tissues	74
Appendix B: Expression profile of PvGGT1 and PvGGT4 in various plant tissues.	75
Appendix C: Multiple sequence alignment of <i>EcGGT</i> , <i>HpGGT</i> and PvGGT1, PvGGT4.	76
Appendix D: PvGGT1 primers for RT-PCR experiment align with transcripts of PvGGT1.	77
Appendix E: PvGGT4 primers for RT-PCR experiment align with transcripts of PvGGT4.	78

List of Abbreviations

APR	APS reductase
APS	Adenosine 5'-phosphosulfate
ATPS	ATP sulfurylase
BSAS	β -substituted alanine synthase
BSO	Buthionine sulfoximine
CAS	Cyanoalanine synthase
CBL	Cystathionine β -lyase
CBS	Cystathionine β -synthase
CDS	Coding sequence
CFP	Cyan fluorescent protein
CGS	Cystathionine γ -synthases
CS	Cysteine synthase
cTP	Chloroplast transit peptide
Cys	Cysteine
DTT	Dithiothreitol
GCL	Glutamate-cysteine ligase
GGT	γ -Glutamyl transpeptidase
GS	Glutathione synthetase

GSH	Glutathione
GST	Glutathione- <i>S</i> -transferase
hGSH	Homoglutathione
HPLC	High-Performance Liquid Chromatography
HRMS	High Resolution Mass Spectrometry
IC ₅₀	Half maximal inhibitory concentration
IPTG	Isopropyl β -D-1 thiogalactopyranoside
K _i	Inhibition constant
K _m	Michaelis constant
LB	Luria-Bertani medium
MES	2-(N-morpholino) ethanesulfonic acid
Met	Methionine
MGL	Methionine- γ -lyase
MOPSO	β -Hydroxy-4-morpholinepropanesulfonic acid
MS	Mass spectrometry
MT	Methyltransferase
NEM	N-ethylmaleimide
OAS	<i>O</i> -acetylserine
OAS-TL	<i>O</i> -acetylserine (thiol) lyase

OD	Optical density
OMT	<i>O</i> -methyltransferase
OPH	<i>O</i> -phosphohomoserine
PAPS	3' phosphoadenosine 5' phosphosulfate
PNA	<i>p</i> -nitroanilide
Pv	Phaseolus vulgaris
PvGEA	Common Bean Gene Expression Atlas and Network Analysis
RFP	Red fluorescent protein
RT	Room temperature
S	Sulphur
<i>S</i> -methylCys	<i>S</i> -methyl-cysteine
<i>S</i> -methylhGSH	<i>S</i> -methylhomoglutathione
SAM	<i>S</i> -adenosylmethionine
SDS-PAGE	Sodium Dodecyl Sulfate-Polyacrylamide Gel Electrophoresis
Ser	Serine
SERAT	Serine acetyltransferase
SiR	Sulfite reductase
SMM	<i>S</i> -methylmethionine
SSPs	Storage seed proteins

TAIR	The Arabidopsis Information Resource
Thr	Threonine
V _{max}	Maximum reaction rate
YFP	Yellow fluorescent protein
γ -Glu-Cys	γ -Glutamylcysteine
γ -Glu- <i>S</i> -methylCys	γ -Glutamyl- <i>S</i> -methylcysteine
γ -GPNA	γ -Glutamyl- <i>p</i> -nitroanilide

Chapter 1

1 Introduction

1.1 Common bean

Common bean (*Phaseolus vulgaris*) is one of the most consumed food legume crops worldwide, plays an essential role in developing countries and contributes half of the grain legume consumption for humans (McClellan et al., 2004). Especially in the Caribbean, and Central and South America, common bean has an average contribution of approximately 9 kg/per capita/year (FAO, 2014). Beans are the primary dietary protein supply in some countries such as Mexico and Brazil (Broughton et al., 2003). Among the families of pea and bean plants, common bean is eaten the most compared to other legumes, and contain approximately 16-33% protein (Broughton et al., 2003). Besides being a good source of protein and fibre, common bean is also recognized as a functional food to provide health benefits and prevent human diseases (De Ron et al., 2015). The inclusion of common bean as part of the diet is associated with a significant reduction of risk of non-transmissible diseases such as obesity, cardiovascular diseases, and many types of cancers (De Ron et al., 2015; Luna-Vital et al., 2015). The important fiber and starch content in common bean may contribute to these health benefits (De Ron et al., 2015).

1.2 Seed storage proteins

The storage proteins in dry seed of common beans are important protein resources for humans (Krishnan, 2000). The main function of seed storage proteins (SSPs) is to accumulate nitrogen, carbon and sulphur as a storage sink. They serve as a major source of reduced nitrogen in early seedling growth (Krishnan, 2000). The major part of legume seed is the cotyledon, which synthesizes about 95% of the storage proteins during the expansion growth phase (De Ron et al., 2015). Cotyledons contain about 16% protein during developing stages and about 20% at maturity (De Ron et al., 2015). There are two major storage proteins in common beans, oligomeric globulins and albumins (De Ron et al., 2015). Globulin storage proteins include 7S and 11S according to

their sedimentation coefficients, they are also commonly known as vicilins and legumins, respectively (De Ron et al., 2015). The 7S globulin phaseolin is the most abundant SSP in common beans, and it constitutes up to 50% of the total seed proteome (De Ron et al., 2015). On the other hand, the 11S globulin is only a minor protein component of common beans and accounts for 3% of seed protein (Derbyshire, 1976). Albumin proteins play an important role in the physiology of the plant and are involved in a protective system that resists insects, predators and various stress conditions in the seed (Chrispeels & Raikhel, 1991).

Lectins are proteins containing a non-catalytic domain that binds to a specific carbohydrate. They are also considered as storage proteins in plants (Cândido et al., 2011). Lectins are involved in biological processes that protect plant tissue, such as antimicrobial/antiviral action (Cândido et al., 2011). The amino acid profile shows legume storage proteins are rich in essential amino acids but have low amount of essential *S*-amino acids (i.e. methionine and cysteine) and tryptophan (De Ron et al., 2015).

1.3 Protein quality and sulphur metabolites

Although being the third most important food legume worldwide next to soybean and peanut and contributing 15% of world protein requirement, the protein quality in common bean and many other grain legumes is not optimal (De Ron et al., 2015; Kalavacharla et al., 2011). The primary reason for suboptimal protein quality is low concentration of sulphur amino acids, cysteine (Cys) and methionine (Met) (Sgarbieri & Whitaker, 1982). Since methionine cannot be synthesized by human and other animals, it is one of the essential amino acids. (Ferla & Patrick, 2014). In contrast, plants are able to synthesize methionine and consuming methionine-containing food is important in human diet (Ferla & Patrick, 2014).

In the main storage protein 7S globulins, the level of methionine and cysteine is particularly low (De Ron et al., 2015). In common bean, the sum of these two sulphur amino acids is considered as one of the most important factors when evaluating protein quality (FAO, 2013). In plants, sulphur is essential for numerous biological activities despite being the least abundant macroelement (Leustek et al., 2000). Cysteine is responsible for the synthesis of most sulphur-containing

compounds in plants (Leustek et al., 2000). In fact, the concentration of cysteine and methionine in the seed of common bean may be limited due to the accumulation of large amounts of a γ -glutamyl dipeptide of the nonprotein amino acid *S*-methylCys (Taylor et al., 2008). The dipeptide, γ -Glu-*S*-methylCys, is a storage form of sulphur and cannot provide the dietary benefit of proteinogenic sulphur amino acids (Taylor et al., 2008). It takes up to 0.3% of dry seed weight of common bean and can account for most of the total *S*-methylCys in mature seeds (Saboori-Robat et al., 2019; Taylor et al., 2008). *S*-methylhomoglutathione (*S*-methylhGSH) is another *S*-amino acid derivative involved in the non-protein sulphur amino acid biosynthetic pathway. It was predicted to be the major intermediate in the biosynthesis of γ -Glu-*S*-methylCys in previous studies (Joshi et al., 2019b). **Figure 1.1** shows the chemical structure of the protein sulphur amino acids, non-protein sulphur amino acid and its γ -glutamyl dipeptide, and the putative major intermediate *S*-methylhGSH.

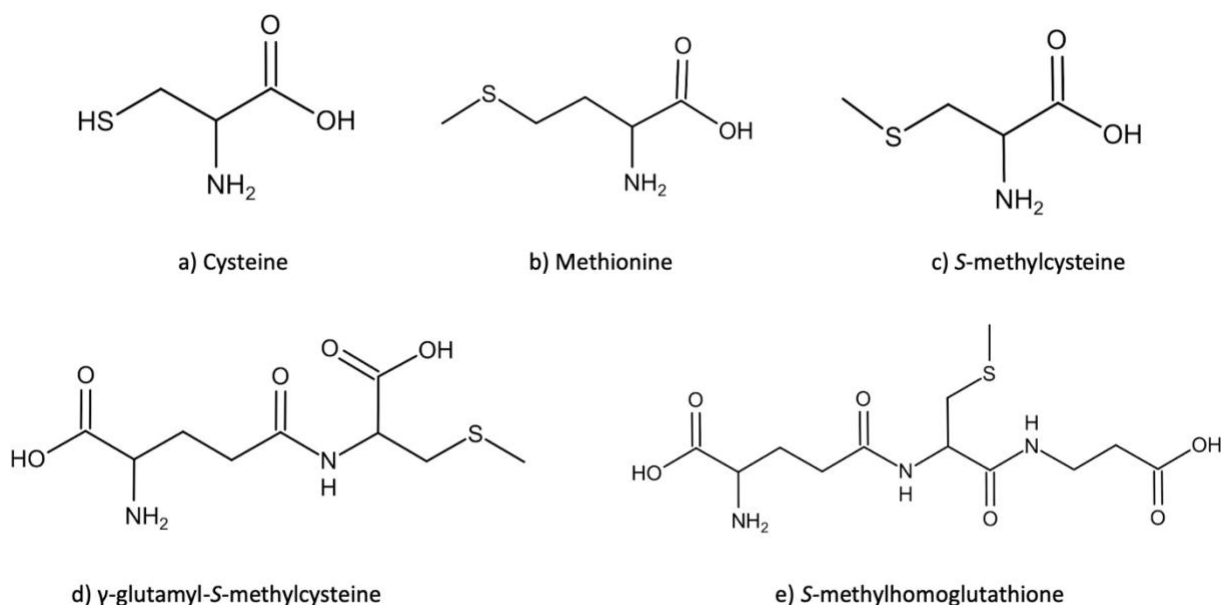


Figure 1.1: The chemical structures of sulphur containing amino acids and *S*-derivatives in *Phaseolus. vulgaris*.

1.4 Sulphur metabolism in plants

Sulphur is an essential element in the ecosystem, and exists in nature in both organic and inorganic forms. The most oxidized form of sulphur, sulfate (SO_4^{2-}), is the primary sulphur source for plants to utilize and incorporate into organic metabolites (Takahashi et al., 2011). A large amount of research on sulphur metabolism has taken place in the plant model, *Arabidopsis thaliana*. The process of assimilation of sulfate in plant metabolism includes activation of sulfate within the cell, reduction of sulfate to sulfide and biosynthesis of cysteine (Buchner et al., 2004).

Sulfate influx is mostly mediated by proton/sulfate cotransporter and driven by proton gradient across the plasma membrane in plants (Takahashi et al., 2011). To activate sulfate, ATP sulphurylase (ATPS) (EC: 2.7.7.4) is required to catalyze a process called adenylation to form adenosine 5'-phosphosulfate (APS) (Takahashi et al., 2011). APS can be reduced to sulfite (SO_3^{2-}) by APS reductase (APR) (EC: 1.8.99.2) or further phosphorylated to form 3'-phosphoadenosine 5'-phosphosulfate (PAPS) to be used in sulfation reactions (Takahashi et al., 2011).

Sulfate reduction exclusively occurs in the plastids in all photosynthetic organisms except *Euglena gracilis* (Brunold & Schiff, 1976). Sulfite synthesized from APS can be further reduced to sulfide (S^{2-}) by ferredoxin dependent sulfite reductase (SiR) (EC: 1.8.7.1), which depends on FeS centers and siroheme as prosthetic groups (Krueger & Siegel, 1982).

Sulfide is the substrate for cysteine synthesis, in a two-step process. At first, serine is recruited to form *O*-acetylserine (OAS) using coenzyme A. Secondly, the enzyme in β -substituted alanine synthase (BSAS) family, *O*-acetylserine (thiol) lyase (OAS-TL), catalyzes the reaction in which sulfide is exchanged for the acetyl moiety from OAS to produce cysteine (Dahl et al., 2008). The process of assimilation of sulfate to produce cysteine in plant metabolism is presented in **Figure 1.2**.

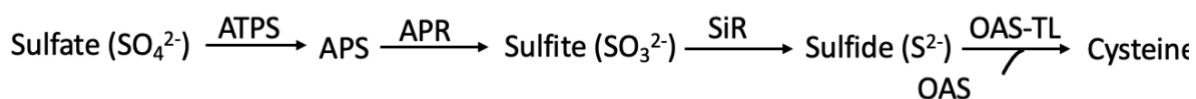


Figure 1.2 Simplified model of the sulphur assimilation to synthesize cysteine in plants.

1.5 Cysteine as a metabolic precursor

After being generated from OAS, cysteine can be used as a precursor to produce a wide range of primary and secondary sulphur containing metabolites (Takahashi, 2010). Glutathione (γ -Glu-Cys-Gly; GSH) is one of the secondary metabolites synthesized from cysteine in two ATP-dependent reactions, which involves γ -glutamylcysteine (γ -Glu-Cys) as an intermediate. In the first reaction, γ -Glu-Cys is synthesized using glutamate and cysteine as substrates catalyzed by glutamate-cysteine ligase (GCL; EC 6.3.2.2) (Takahashi et al., 2011). Cysteine and glutamate are joined by an amide linkage between α -amino group and γ -carboxyl group (Okada & Kimura, 2022). The biosynthesis of γ -Glu-Cys is considered the rate-limiting step in glutathione synthesis; it depends on the availability of the fully oxidized form of GCL (Hell & Bergmann, 1990). There is feedback inhibition of GCL by glutathione, which acts as a demand-driven control of this pathway (Takahashi et al., 2011). Buthionine sulfoximine (BSO) is a specific and potent inhibitor of GCL (Griffith & Meister, 1979). BSO is an analog of the enzyme-substrate complex formed in the transition state of the reaction, and results in irreversible inhibition (Meister, 1995).

In the second reaction, glutathione synthetase (GS; EC: 6.3.2.3) catalyzes the reaction to yield glutathione by adding glycine to the C-terminal site of γ -Glu-Cys (Hell & Bergmann, 1990). Unlike other plants, homogluthathione (hGSH; γ -Glu-Cys- β -Ala) is the major storage form of reduced sulphur in legumes instead of glutathione (Matamoros et al., 1999). Glutathione plays an important role in cellular defense against oxidative stress, control of redox status, detoxification, and plant growth and development (Hell & Bergmann, 1990; Matamoros et al., 1999).

Apart from being converted to glutathione, cysteine is also the precursor for methionine biosynthesis. In the first step, cystathionine is synthesized from cysteine and *O*-phosphohomoserine (OPH) catalyzed by cystathionine γ -synthase (CGS) (Takahashi et al., 2011). Then β -cleavage of cystathionine by cystathionine β -lyase (CBL) produces homocysteine, which is further methylated to generate methionine by methionine synthase (MS) (Takahashi et al., 2011). From this point, the majority of cellular methionine is used to form the universal methyl donor, *S*-adenosylmethionine (SAM); the remainder of cellular methionine contributes to protein synthesis (Giovanelli et al., 1980).

1.6 Biosynthesis of sulphur amino acid derivatives

A considerable amount of assimilated sulphur is used to synthesize sulphur amino acid derivatives in some plants, which potentially act as a sulphur storage sink. γ -Glu-*S*-methylCys is likely to be the end-product of non-protein sulphur amino acid biosynthetic pathway (**Figure 1.3**). Some sulphur amino acid derivatives involved in the biosynthesis of γ -Glu-*S*-methylCys include *S*-methylCys and *S*-methylGSH.

S-methylCys is an analogue of methionine and cysteine; it can be used as a substrate in metabolic reactions in place of methionine and cysteine in many species (Rathbun, 1967). There are two major biosynthetic pathways to *S*-methylCys. First, the methylation of cysteine to form *S*-methylCys was reported in radish (Thompson & Gering, 1966). Another mechanism involves OAS and methanethiol as substrates to produce *S*-methylCys via condensation (Husain et al., 2010). The initial step of methionine degradation catalyzed by methionine γ -lyase (MGL) converts methionine into methanethiol, α -ketobutyrate and ammonia (Rébeillé et al., 2006). In *Arabidopsis*, part of the methanethiol from methionine cleavage react with an activated form of serine to produce SMC (Rébeillé et al., 2006). In recent studies, Joshi et al. (2019a) showed that free *S*-methylCys solely comes from methionine and serine in developing seed of common bean. One member of the β -substituted alanine synthase family, BSAS4;1, showed a high cysteine synthase activity and catalyzed the synthesis of *S*-methylCys through the use of OAS and methanethiol as substrates (Joshi et al., 2019a). Previous feeding and isotope tracking studies with ^{13}C ^{15}N serine showed

high percentage of incorporation into γ -Glu-Cys, hGSH and *S*-methylhGSH, which suggested a high metabolic flux from serine to these downstream metabolites (Joshi et al., 2019a).

There are two proposed biosynthetic pathways leading to γ -Glu-*S*-methylCys, the dipeptide of *S*-methylCys. One suggests the synthesis of γ -Glu-*S*-methylCys uses *S*-methylCys as substrate catalyzed by γ -Glu-Cys synthetase (Joshi, 2017). The other one involves the transfer of γ -glutamyl from hGSH to free *S*-methylCys by γ -glutamyl transpeptidase (GGT; EC 2.3.2.2) to form γ -Glu-*S*-methylCys similar to that described for the biosynthesis of *S*-alk(en)yl-L-cysteine sulfoxides in garlic (Yoshimoto et al., 2015). In garlic, the hydrolysis of γ -glutamyl group from the intermediate γ -glutamyl-*S*-alk(en)yl-L-cysteine leads to the production of *S*-alk(en)yl-L-cysteine sulfoxides (Yoshimoto et al., 2015). GGT consists of one small (β) and one large (α) subunit, about 20 kDa and 40 kDa respectively (Suzuki & Kumagai, 2002). An intramolecular autocatalytic event separates GGT into β -subunit and α -subunit, and the cleavage site is a strictly conserved threonine (Suzuki & Kumagai, 2002). The function of GGT is to remove γ -glutamyl group from γ -glutamyl compounds and transfer it to other amino acids, peptides and water (Tate & Meister, 1981). Both *S*-methylCys and γ -Glu-*S*-methylCys are non-proteinaceous amino acids and they abundantly accumulate in the seed of *P. vulgaris*.

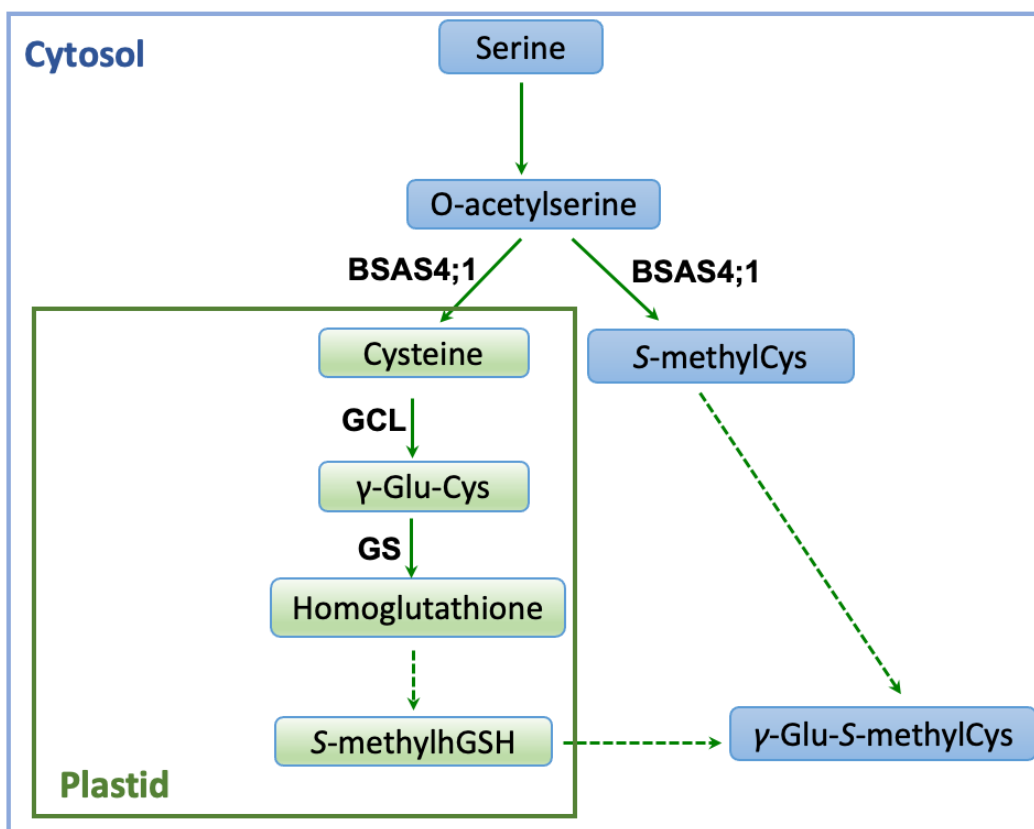


Figure 1.3. Biosynthetic pathway of non-protein sulphur amino acids in the developing seed of common bean.

Solid lines in this simplified scheme indicate sulphur metabolism reported in other studies; while dashed lines indicate putative reactions for metabolite synthesis (Joshi et al., 2019a).

Glu: glutamyl; Cys: cysteine; BSAS: β -substituted alanine synthase; GCL: glutamyl-cysteine ligase; hGSH: homogluthathione; GS: glutathione synthase.

1.7 Potential methods to improve protein quality in legumes

In the last five decades, efforts have been made toward improving the quality of seed storage proteins in legumes. Early focus of this research was on traditional breeding by working with mutant lines to increase seed protein concentration and rebalance proteome thus improving essential amino acid levels (Bliss & Brown, 1983). Sullivan's (1981) work to improve quantity and quality of seed protein in common bean is an example of inbred backcross breeding method. The best genetic lines were selected after backcrossing with one of the high protein inbred backcross families, Sanilac, and a few generations of selfing (Sullivan, 1981). Sanilac was used as a recurrent cultivar parent in many other studies. Additionally, inbred backcross method was also used to enhance genetic resistance to some diseases (Bliss & Brown, 1983).

Phaseolin and phytohemagglutinin are both important seed storage proteins. Osborn et al. (2003) reported two genetic lines, SMARC1N-PN1 and SMARC1-PN1, which are deficient in phaseolin and phytohemagglutinin. Furthermore, Taylor et al. (2008) showed that methionine was 10% and cysteine 70% higher in these two lines at the expense of the abundant non-protein amino acids, *S*-methylCys. When comparing the gene expression of SMARC1N-PN1 (mutant line) to SARC1 (wild-type line), more activated cytosolic OAS was observed for cysteine synthesis due to up-regulation of two cytosolic serine *O*-acetyltransferases (*SERAT1;1* and *SERAT1;2*); while the decrease in total *S*-methylCys biosynthesis might be related to down-regulation of a plastidic serine *O*-acetyltransferase (*SERAT2;1*) (Liao et al., 2012).

More recently, research has been shifted to transgenic approaches to modify protein composition or engineer sulphur amino acid pathways (De Ron et al., 2015; Liao et al., 2012). For example, manipulation of the expression of genes that encodes methionine-rich Brazil nut (*Bertholletia excelsa*) 2S albumin protein, which contains more than ten times the amount of methionine compared to most proteins (Altenbach et al., 1987). Later, Aragão et al. (1999) increased the methionine content in *P. vulgaris* up to 23% by manipulating promoter and enhancer sequences of one of the Brazil nut's 2S-albumin genes. Overexpression of Gm2S-1 gene in soybean and other legumes is another example of transgenic approach to improve nutritional quality of protein (Galvez et al., 2008). The Gm2S-1 gene encodes a novel methionine-rich protein in soybean that

contains about 8% methionine and significantly higher lysine and cysteine than other proteins (Galvez et al., 2008). This genetic research is in progress to evaluate whether the mutant line could be used for protein quality improvement.

1.8 Research objectives

The long-term goal of this research is to redirect assimilated sulphur in seeds into increased biosynthesis of sulphur amino acids, cysteine and methionine, and improve the nutritional quality of legumes. The accumulation of large amounts of γ -Glu-*S*-methylCys in the seed of common bean is associated with suboptimal levels of cysteine and methionine (Sgarbieri & Whitaker, 1982). The major aim of this study is to understand the biosynthetic pathway of γ -Glu-*S*-methylCys including the key intermediate *S*-methylhGSH, which can help with redirecting sulphur assimilation to the synthesis of sulphur amino acids.

The objectives of this study were as follows:

1. To reveal the mechanism of the biosynthesis of *S*-methylhGSH.

This study used both ^{13}C -sodium thiomethoxide and ^{34}S -methionine feeding and isotope label tracing in downstream compounds using high resolution mass spectrometry (HRMS).

2. To characterize potential substrates involved in this biosynthesis of γ -Glu-*S*-methylCys.

This study focused on identifying the substrates for producing γ -Glu-*S*-methylCys by using soluble protein extracts from seeds in biochemical assays. HPLC was used to identify metabolites. Subcellular localization of candidate γ -glutamyl transferase was also performed to learn about the subcellular compartmentation in γ -Glu-*S*-methylCys biosynthesis.

3. To characterize the inhibition of the biosynthesis of *S*-methylCys by benzoic acid.

Based on the evidence of the crystal structure of benzoic acid binding to the enzyme PvBSAS4;1, which catalyzes the synthesis of *S*-methylCys, the inhibitory effect of benzoic acid was studied in biochemical and kinetic assays.

Chapter 2

2 Materials and methods

2.1 Plant material and growth conditions

The genotype BAT93 of common bean (*P. vulgaris*) was grown in growth cabinets (Convicon, Winnipeg, MB, Canada) with a cycle of 16 h light (300-400 $\mu\text{mol photons m}^{-2} \text{s}^{-1}$) at 24 °C and 8 h dark at 18°C. Seeds were germinated in small pots (8 × 10 cm) with vermiculite, and seedlings were transplanted to larger pots (17 × 20 cm) with Promix BX soil (Premier Tech Horticulture, Rivière-du-Loup, Québec, Canada). Plants were fertilized with 0.75 g 20:20:20 (N:P:K) fertilizer per pot once a week after transplantation.

2.2 Determination of the mechanism of the biosynthesis of S-methylhGSH

2.2.1 Chemicals

³⁴S-labeled methionine and ¹³C-labeled sodium thiomethoxide were purchased from Toronto Research Chemicals (Toronto, Ontario, Canada). Other chemicals were obtained from Sigma-Aldrich (Oakville, Ontario, Canada).

2.2.2 Candidate genes for S-methylhomoglutathione synthesis

To identify all the members of the glutathione-S-transferase (GST) and methyltransferase (MT) family in *P. vulgaris*, an annotation search was performed in the protein database of *P. vulgaris* v2.1 available in Phytozome (www.phytozome.net). Transcript expression profiles of each gene in different plant tissues are reported in PvGEA (PvGEA: Common Bean Gene Expression Atlas and Network Analysis (zhaolab.org)), and expression values are represented as RPKM (reads per kilobase of transcript per million mapped reads) (O'Rourke et al., 2014). Initial screening was based on specificity of seed expression and the level of expression in young seed tissues. Resulting gene candidates were analyzed with WOLF pSORT (<http://www.genscript.com/wolf-psort.html>)

(Horton et al., 2007) to acquire predicted sub-cellular location. The predicted result of the presence of chloroplast transit peptide (cTP) in ChloroP (<http://www.cbs.dtu.dk/services/ChloroP/>) was also taken into consideration.

2.2.3 Cloning of candidate genes and recombinant protein purification

Expression constructs for selected candidate genes of GST and MT were designed and cloned into the bacterial expression vectors pQE30, constructs were obtained from Biomatik (Kitchener, Ontario, Canada) and transformed into XL10-Gold competent cells (Agilent Technologies, Mississauga, ON).

For protein purification, XL10-Gold cells containing desired plasmid were grown overnight at 37 °C in 5 mL of Luria-Bertani (LB) medium, supplemented with ampicillin (100 µg/mL), and used for inoculation. A 500 mL NZY medium was prepared for cell proliferation. When the OD₆₀₀ of cells reach 0.6, 1 mM isopropyl β-D-1 thiogalactopyranoside (IPTG) was added to induce cells to produce recombinant proteins. After growing in the medium with shaking for 14-16 hours at room temperature, cells were harvested by centrifugation (4 °C, 6,000 × g, 30 min) and stored at -20 °C. After resuspension in His-tag isolation bead binding buffer (20 mM NaH₂PO₄, 0.5 M NaCl, 20 mM imidazole, pH 7.4), cells were lysed with the aid of a French press. Samples were sonicated 10 times for 30 s with 15 s breaks on ice to facilitate release of cellular content. After centrifugation (4 °C, 18,000 × g, 45 min), the resulting supernatant was applied to His-Tag Isolation beads (Cytiva (cytivalifesciences.com)). Impurities and unbound proteins were eliminated with wash buffer (50 mM NaH₂PO₄, 300 mM NaCl, 40 mM imidazole, pH 8.0). Purified protein was collected by washing beads with elution buffer (50 mM NaH₂PO₄, 300 mM NaCl, 250 mM imidazole, pH 8.0), then protein was desalted and concentrated by PD-10 column (GE Healthcare Life Sciences) and Amicon Ultra-15 Ultracel 30 K filter unit (Millipore, Etobicoke, ON) respectively (Maruyama et al., 1998). Protein was stored in small aliquots at -20 °C for enzyme assay.

2.2.4 Seed protein extraction

Twelve to fifteen days after fertilization, seeds between 20-36 mg were collected and stored at -80 °C after flash freezing in liquid nitrogen. Dry bean seeds were ground to a very fine powder and 100 mg was homogenized in cold extraction buffer (50 mM Tris-HCl pH 8.0, 50 mM KCl, 1 mM CaCl₂, 10% glycerol, 1 mM dithiothreitol (DTT)) containing one phosphatase inhibitor tablet (Sigma-Aldrich, Oakville, ON) per 7 mL buffer. To separate soluble protein from plant tissue, samples were centrifuged for 30 min at 4 °C at 16,000 × *g*. The supernatant was then transferred to a fresh tube and centrifuged again for 20 min at 4 °C at 16,000 × *g*. Protein concentration was determined by the Bradford assay (Harlow & Lane, 2006).

2.2.5 Enzyme assays for S-methylhomoglutathione biosynthesis

2.2.5.1 Enzyme assay with GST protein

Enzyme reactions were performed in 100 μL of 20 mM HEPES-KOH (pH 8.0), with 1 mM homoglutathione, 1 mM sodium thiomethoxide and 2 mM DTT. After adding 10 ng purified GST recombinant protein, reaction mixtures were incubated for 2 h at 30 °C. Soluble protein from seed extract was also used as a source of enzyme. To terminate the reaction, 50 μL of 40 mM HCl was added to each reaction mixture. To identify the presence of target product, samples were filtered through 1.2 μm filters (Pall Life Sciences, Mississauga, ON) before transferring to amber glass HPLC vial and analyzed by HPLC.

2.2.5.2 Enzyme assay with MT protein

Possible methyl donors in this reaction are *S*-adenosylmethionine (SAM), *S*-methylmethionine (SMM), methyltetrahydrofolate and trimethylglycine. Separate reaction mixtures with a final volume of 100 μL containing 1 mM of one possible methyl donor along with 1 mM homoglutathione, 2 mM DTT, 20 mM HEPES-KOH (pH 8.0) and 10 ng MT recombinant protein was incubated for 2 hours at 30 °C. Soluble protein from seed extract was also used as a source of enzymes. To terminate the reaction, 50 μL of 40 mM HCl was added to each reaction mixture. Samples were analyzed by HPLC to identify the presence of target product (Joshi, 2017).

2.2.6 Embryo culture and culture media

Common bean pods were harvested 12-15 days after fertilization. Pods were surface sterilized with 0.5% bleach and a few drops of diluted soap (Alconox powdered precision cleaner, Alconox, NY, USA), followed up with three washings in sterile Milli-Q water for 5 min. Developing seeds between 20-36 mg were selected, their seed coats removed and the cotyledons transferred to 6-well surface treated culture plates (VWR, International, Mississauga, ON). Each well contained 2.5 mL of filter-sterilized growth media and six cotyledons from three seeds (Joshi, 2017).

Basic culture media composition followed Joshi et al. (2019a) with minor revision, which contained 8 mM MgSO₄, 10 mM KCl, 3 mM CaCl₂, 1.25 mM KH₂PO₄, 0.5 mM MnSO₄, 0.15 mM ZnSO₄•7H₂O, 0.1 mM sodium EDTA ferric salt, 0.1 mM H₃BO₃, 27 μM glycine, 2.5 μM CuSO₄•5H₂O, 5 μM KI, 1 μM Na₂MoO₄, 0.1 mM CoCl₂•6H₂O, 4 μM nicotinic acid, 1 μM thiamine-HCl, 0.5 μM pyridoxine-HCl, 0.56 mM myo-inositol, 0.1 mM Na₂EDTA, 5 mM MES, 146 mM sucrose and 62.5 mM glutamine. The pH of the culture media was adjusted with KOH to 5.8.

2.2.7 Isotope labelling treatment groups

To track the path of sulphur from methionine and carbon from sodium thiomethoxide to other S-containing metabolites, developing seeds at stage IV were incubated with ³⁴S-methionine or ¹³C sodium thiomethoxide. There were five treatment groups based on basic culture media: labeled methionine supplementation, non-labeled methionine supplementation, labeled sodium thiomethoxide supplementation, non-labeled sodium thiomethoxide supplementation and no supplementation. Isotope compounds were supplied at a concentration of 8 mM. Six cotyledons in each well of culture plates were grown under continuous light and slow shaking (60 rpm) for 48 h at room temperature in each treatment group. Cotyledons were washed with filter-sterilized Milli-Q water three times to remove excessive labeled compounds on the surface. Then, seeds were dried with Kimwipes and stored at -80 °C after flash freezing in liquid nitrogen for future analysis.

2.2.8 Amino acid extraction and mass spectrometry analysis

Amino acid extraction and HPLC analysis were performed to measure the level of metabolites containing isotope label in seed samples. The frozen seeds from section 2.2.7 were homogenized using TissueLyser II (Qiagen) with ceramic beads in 1.5 mL Eppendorf tubes. Extraction buffer (50 mM ammonium bicarbonate in ethanol, pH 5.6) was added to ground seeds, followed by vortexing and sonication to extract soluble metabolites. Samples were treated with 2 mM DTT for 30 min at 45 °C to break disulfide bonds formed between metabolites. Because disulfide bonds are reversible, 6 mM of N-ethylmaleimide (NEM) was added to samples to prevent cleaved bonds to reform. To quench remaining NEM, additional 2 mM DTT was added to the samples. The supernatant was collected after centrifugation (10,000 × *g* at 4 °C, 10 min) and transferred to an amber glass HPLC vial after being filtered through 0.45 μm PTFE syringe filter.

MS data were obtained with a Thermo® Q-Exactive Orbitrap mass spectrometer coupled to an Agilent 1290 HPLC system. Methods for MS/MS and LC-DDA, along with the method used to analyze data on Xcalibur™ software were followed as described (Joshi, 2017). The incorporation percentage of labelled compounds was calculated by determining the ratio of signal intensity of labelled compounds to the sum of labeled and unlabeled signal intensity.

2.3 The biosynthesis of γ -Glu-S-methylCys

2.3.1 Chemicals

γ -Glutamyl-*p*-nitroanilide (γ -GPNA) and *p*-nitroanilide (PNA) were purchased from Sigma-Aldrich. Glycylglycine was purchased from Amresco (Solon, OH, USA). Homoglutathione (hGSH) and *S*-methylcysteine were purchased from Toronto Research Chemicals and Thermo Scientific (Burlington, ON, Canada), respectively.

2.3.2 Plant materials

For subcellular localization studies, *Nicotiana benthamiana* plants were grown in growth cabinets with a cycle of 16 h light (100 $\mu\text{mol photons m}^{-2} \text{s}^{-1}$) at 22 °C and 8 h dark at 20°C. Seeds were germinated in Promix BX soil and transferred to pots (8 × 10 cm) after two weeks. Plants were watered and fertilized regularly with 0.25 g/L 20-8-20 fertilizer. Six-week-old plants were used for infiltration for transient expression.

2.3.3 Candidate genes for γ -glutamyl transferases

Candidate genes search for γ -glutamyl transferases (GGT) was performed in Phytozome (www.phytozome.net) based on gene annotation in the genomic database of *P. vulgaris* v2.1. Transcripts Phvul.001G249200.2 (PvGGT1.2) and Phvul.004G173700.2 (PvGGT4.2) were selected for subcellular localization studies.

2.3.4 Cloning of GGT candidate genes for sub-cellular localization

Sequences of PvGGT1.2 and PvGGT4.2 for sub-cellular localization studies were designed with attB1 and attB2 sites for Gateway cloning technique. Gene sequences were synthesized and cloned into pBluescript SK (+) vectors and obtained from Biomatik (Kitchener, Ontario, Canada). The GGT sequences with attB sites were amplified by PCR using Phusion high-fidelity DNA polymerase (Thermo Fisher Scientific). The primers for PvGGT1.2 were: Fw: 5'-GGGGACAAGTTTGTACAAAAAAGCAGGCTTCATGCCAAGTGTTGCAGCTGT-3' and Rvs: 5'-CCCCTGGTGAAACATGTTCTTTCGACCCAGTTAAAAGCCTGCAGGAAGAC-3';

primers for PvGGT4.2 were: Fw: 5'-GGGGACAAGTTTGTACAAAAAAGCAGGCTTCATGAGAAGCAGTAAGGGAG-3' and Rvs: 5'-CCCCTGGTGAAACATGTTCTTTCGACCCAGAACAGCAGCTGGACATCCAC-3'. The attB sites are underlined. The PCR products were electrophoretically separated on a 1% (w/v) agarose gel and bands corresponding to *PvGGT* size were purified from gel using DNA Gel Extraction Kit (New England Biolabs, Whitby, ON). The purified fragments with attB1 and attB2 sites were recombined with the entry vector pDONR-Zeo (Thermo Fisher Scientific) using BP clonase reaction mix following Gateway cloning methods. The BP reaction product was transformed into *E. coli* XL10-Gold cells by heat shock and cells grown on LB plates containing zeocin (50 µg/mL). Colonies were screened by restriction digest (pDONR-Zeo-PvGGT1 with *EcoRV*; pDONR-Zeo-PvGGT4 with *PciI*). The LR reaction was performed after confirmation using entry clone pDONR-Zeo-PvGGT and destination vector pEarleyGate101 (Invitrogen, USA) by LR clonase reaction mix (Invitrogen, USA). Destination clone was transformed into *E. coli* XL10-Gold cells and cells grown on LB plate supplemented with kanamycin (50 µg/mL). After confirming colonies with positive clones by restriction digest (pEG101-PvGGT1 with *EcoRV*; pEG101-PvGGT4 with *HindIII*), the plasmid DNA carrying the 'destination clone', pEG101-PvGGT was transformed into *Agrobacterium tumefaciens* strain GV 3101 for infiltration.

2.3.5 Transient expression and confocal microscopy

The transient expression of the plasmid (pEG101-PvGGT) fused to yellow fluorescent protein (YFP) in *A. tumefaciens* strain GV3101 was performed on the *N. benthamiana* leaf by infiltrating into leaf epidermal cells (Sparkes et al., 2006). The first step was to inoculate a single colony in the medium (LB broth containing 10 mM 2-(N-morpholino) ethanesulfonic acid [MES] pH 5.6, and 100 µM acetosyringone) containing rifampicin (25 µg/mL), kanamycin (50 µg/mL), and gentamycin (50 µg/mL) and grown at 28 °C with shaking (250 rpm) until the OD₆₀₀ reached 0.6. The pellet was collected and resuspended in Gamborg's solution (3.2 g/L Gamborg's B5 medium with vitamins, 20 g/L sucrose, 10 mM MES pH 5.6, and 200 µM acetosyringone) after centrifuging the culture at 3,000 × g for 30 min at RT. To activate the virulence gene required for transformation, cell culture in Gamborg's solution was incubated for 1 h at RT when the OD₆₀₀ reached 1. To verify subcellular localization of PvGGT1.2, several organelle marker proteins were used

including nuclear (H2B-RFP), Golgi (NbNBR1-CFP) and mitochondrial (cytochrome oxidase-CFP) markers (Li et al., 2020; Tang et al., 2022). H2B-RFP and NbNBR1-CFP are proteins expressed in transgenic *N. benthamiana*, described in Li et al. (2020). Cells with plasmid DNA carrying pEG101-GGT were mixed with each organelle markers in a 1:1 ratio and coexpressed in *N. benthamiana* leaves (Nelson et al., 2007).

To infiltrate leaves, bacteria were slowly injected into the abaxial side of the leaf of 4-5-week-old *N. benthamiana* plants using a 1 mL syringe. Epidermal cell layers of *N. benthamiana* leaves were visualized using an OLYMPUS FV1200 confocal microscope with a 60 × water immersion objective. Excitation wavelengths for YFP, CFP and RFP were 514, 458 and 543 nm, respectively, while their emission spectra were 565-585, 470-500 and 590-630 nm. Chlorophyll autofluorescence was recorded at 680-720 nm emission to study the expression of GGT in chloroplast (Wei et al., 2010). For co-localization study, the expression of GGT and marker proteins was recorded at different excitation wavelengths sequentially by using the ‘Sequential Scan Tool’.

2.3.6 Cloning for recombinant protein expression and purification

Constructs for recombinant protein expression of GGT genes were designed and cloned into the bacterial expression vectors pQE30. Constructs were obtained from Biomatik. Initial crude γ -glutamyl transferase recombinant protein isolation followed the methods described in section 2.2.3. Instead of using His-tag isolation beads, crude recombinant protein was purified by HisTrap His-tag protein purification column (Cytiva, Sweden) using an ÄKTA pure system (Cytiva). The HisTrap column was equilibrated with binding buffer (20 mM NaH₂PO₄, 0.5 M NaCl, 20 mM imidazole, pH 7.6), washed with wash buffer (50 mM NaH₂PO₄, 300 mM NaCl, 40 mM imidazole, pH 7.6), and proteins were eluted with elution buffer (50 mM NaH₂PO₄, 300 mM NaCl, 250 mM imidazole, pH 7.6) at a flow rate of 5.0 mL/min. Purified protein was desalted and concentrated by PD-10 column and Amicon Ultra-15 Ultracel 30 K filter unit, respectively.

2.3.7 Soluble protein extraction from developing seeds

Soluble protein from developing seeds of *P. vulgaris* was extracted and used as a source of enzyme in GGT enzyme assay. Developing seeds between 16-36 mg were collected and flash frozen in liquid nitrogen. Frozen seeds were homogenized in liquid nitrogen using mortar and pestle. Five gram of seed flour was added to 60 mL Tris-HCl buffer (pH 7.6) containing 5 mM β -mercaptoethanol and 1 mM EDTA. The mixture was vortexed and stirred thoroughly before centrifugation ($8000 \times g$, 4 °C, 20 min). The supernatant was collected and precipitated by 30% ammonium sulfate $[(\text{NH}_4)_2\text{SO}_4]$, then centrifuged at $8000 \times g$, 4 °C for 20 min. The supernatant was further isolated by HiTrap Phenyl Sepharose HP column (Cytiva) using an ÄKTA pure system. The column was equilibrated with 50 mM Tris-HCl buffer (pH 7.6) containing 1 M $(\text{NH}_4)_2\text{SO}_4$. Sample was eluted with 50 mM Tris-HCl buffer (pH 7.6) at a flow rate of 2.0 mL/min. Fractions were pooled based on UV peaks on chromatogram (Li et al., 2012). The concentration of fractions was measured by NanoDrop 1000 (Thermo Fisher Scientific).

2.3.8 Assay of GGT activity

The activity of GGT in fractions from section 2.3.7 was measured following the method described by Iwami et al. (1975) with a few modifications. The assay was performed in 200 μL of 50 mM Tris-HCl (pH 7.6), 5 mM γ -GPNA and 5 mM glycylglycine in 96-well microtiter plate. Samples were prepared in duplicate. Reactions were started by adding 5 μg protein from fractions followed by incubation at 37 °C for 1 h. GGT catalyzes the hydrolysis of γ -glutamyl-*p*-nitroanilide (γ -GPNA) to produce *p*-nitroaniline (PNA), which is yellow in color and can be easily detected by spectrometry. The assay with γ -GPNA was used to determine the activity of GGT enzyme. The production of *p*-nitroaniline was monitored by spectrophotometry at 410 nm with a Power Wave XS 96-well plate reader (Bio-Tek instruments, Winooski, VT).

2.3.9 Enzyme assay

Enzyme reactions were performed in 100 μL of 50 mM Tris-HCl (pH 7.6), with 1 mM homogluthathione (hGSH) and 0.3 mM *S*-methylcysteine (SMC) as substrates in a 1.5 mL Eppendorf tube. Reactions were started with 5 μg seed extract from fractions described in section 2.3.7, then incubated for 1 h at 37 °C. To detect the formation of γ -glutamyl-*S*-methylCys, reaction

mixtures were analyzed by HPLC after filtering through an Amicon Ultra-15 Ultracel 30 K filter unit to remove residual proteins.

2.3.10 RT-PCR

To further confirm the presence of different transcripts of GGT in developing seeds of *P. vulgaris*, RT-PCR was performed. Primers were designed based on the transcript sequences of *PvGGT1* and *PvGGT4* in *P. vulgaris* v2.1 available in Phytozome. The primer sequences for two transcripts of *PvGGT1* were: Fw, 5'- TGAGTGTGTGTGTGTCACTA -3'; and Rvs, 5'- GGAATCCAATTGATGTGGTT-3'. There are common forward and reverse primers for five transcripts of *PvGGT4*, which were: Fw, 5'-GCCAAACCAAACTGAGCTG -3'; and Rvs, 5'- TGTCTGGCATGGTATAGATC-3'. To better distinguish transcript sequences with high similarity, specific primers were also designed for RT-PCR experiment. The specific forward primer for transcript *PvGGT4.3* was 5'-CAAGAAGTTGGGAACCACCA -3'; and the specific reverse primer for transcript *PvGGT4.4* was 5'- CCCTGGGAGTGATGAATAAA -3'.

Total RNA extract from BAT93 was prepared by a former NSERC Visiting Fellow Dengqun Liao (Liao et al., 2012) and treated with DNase I to minimize DNA contamination. RNA quality was verified by electrophoretic separation on a 1% (w/v) agarose gel. The SuperScript cDNA synthesis kit (Thermo Fisher Scientific) was used to synthesize first-strand cDNA with 2 µg total RNA in a 20 µL reaction. Following this, a 50 µL PCR reaction was performed using Taq DNA polymerase (Thermo Fisher Scientific) and 2 µL of 20-fold dilution of resulting cDNA was used as template. The amplification conditions were denaturation at 95 °C for 2 min; 35 cycles at 95 °C for 2 min; 53 °C for 3 min and 68 °C for 60 s; and a final extension at 68 °C for 10 min. The PCR product was separated by electrophoresis in a 1% (w/v) agarose gel. Bands appearing on the gel were purified using DNA Gel Extraction Kit (New England Biolabs) and sent for Sanger sequencing by using the same primers.

2.4 Characterization of benzoic acid as an inhibitor

2.4.1 Chemicals

¹³C, ¹⁵N isotope labelled serine was purchased from Cambridge Isotope Laboratories (Tewksbury, MA, USA). Other chemicals were obtained from Sigma-Aldrich.

2.4.2 Recombinant protein purification and size-exclusion chromatography

A *PvBSAS4;1* expression construct was prepared by a former PhD student Jaya Joshi (Joshi, 2017). *PvBSAS4;1* recombinant protein purification followed the methods described in section 2.2.3. To further remove impurities in protein samples, size exclusion chromatography was performed on ÄKTA pure system using HiLoad Superdex 200 prep grade column with buffer (100 mM β-Hydroxy-4-morpholinepropanesulfonic acid (MOPSO), pH 7.0). The size of eluted protein was analyzed on a 12% gel by SDS-PAGE. Protein concentration was determined by Bradford assay (Harlow & Lane, 2006).

2.4.3 Biochemical and kinetic assay

To determine the inhibitory effect of benzoic acid on *PvBSAS4;1* enzyme activity, an assay to show the activity of cysteine synthase was performed in the presence and absence of benzoic acid. A broad concentration range (10-2000 μM) of benzoic acid was used at the beginning to determine the optimal concentration for inhibition. A reaction mixture was performed in 100 μL of 100 mM MOPSO (pH 7.0), 8 mM *O*-acetylserine (OAS), 0.75 mM sodium sulfide and varied amount of benzoic acid and was incubated for 20 min at 25 °C. The negative control in this experiment was a reaction without recombinant enzyme; the positive control was a reaction without benzoic acid. Acid ninhydrin reagent was prepared by dissolving 250 mg of ninhydrin in 6 mL acetic acid and 4 mL concentrated HCl. To stop the reaction, an additional 50 μL of 40 mM HCl was added and mixed with an equal amount of premade acid-ninhydrin reagent. As described by Gaitonde (1967), the acid ninhydrin reagent reacts specifically with cysteine in forming a colored product. The production of cysteine was determined with a PowerWave XS plate reader at 560 nm. Enzyme kinetic assays were performed to determine the half maximal inhibitory concentration (IC₅₀) and

the inhibition constant (K_i) of the inhibitor. Reactions were prepared with a series of substrate concentration (2-8 mM of OAS; 0.5-1.2 mM of sodium sulfide) in the absence of inhibitor, as well as in the presence of different concentration of inhibitors (Todd & Gomez, 2001). A Lineweaver-Burk plot was used to determine the type of inhibition of benzoic acid by looking at the V_{max} of the reactions with the change of substrate concentration (Fjellstedtand & Schlesselman, 1977). Dixon plots and slope replots were used to determine K_i , which is the constant describing the binding affinity between the inhibitor and the enzyme (Benjamin & Theodore, 2003). Other molecules that have similar structure as benzoic acid were also used in this biochemical assay as inhibitor candidates, such as salicylic acid, tyrosine, and phenylalanine.

2.4.4 Embryo culture and culture media

Embryo culture was prepared following the methods described in section 2.2.6. Seeds were grown in 6-well surface treated culture plates containing basic culture media, described in section 2.2.6. To determine the optimal concentration of benzoic acid for *in-vitro* incubation, a series of benzoic acid concentration (0 - 1.2 mM) was tested and the appearance and growth in fresh weight of cotyledons was recorded after 48 h incubation. Similarly, a range of buthionine sulfoximine (BSO) concentration (0-2.5 mM) was tested to determine the optimal BSO concentration in feeding experiments. The basic media was supplemented by 8 mM labelled serine and 1.2 mM benzoic acid or 2.5 mM BSO.

2.4.5 Amino acid extraction and MS analysis

To measure the level of isotope labeled compounds after incubation, amino acids were extracted from frozen seeds in extraction buffer and processed for mass spectrometry analysis following the methods described in section 2.2.8.

Chapter 3

3 Results

3.1 Determination of the mechanism of the biosynthesis of *S*-methylhGSH

3.1.1 Tracking the fate of isotope labeled sodium thiomethoxide and methionine

To better illustrate the study of reactions in different sections, Figure 3.1 shows the non-protein amino acid biosynthetic pathway in common bean corresponding to sections in this chapter. To track the path of sulphur from methionine to other *S*-containing metabolites, developing seeds at stage IV were incubated with ^{34}S -methionine (Walbot et al., 1972). The uptake of labeled methionine was determined by high resolution mass spectrometry (HRMS) analysis of seed extracts after 48 h incubation. Most of the *S*-metabolites in the pathway contained isotope labeled sulphur (Figure 3.1). From upstream to downstream of the pathway, the percentage incorporation of ^{34}S in γ -Glu-Cys, homogluthathione (hGSH), *S*-methylhGSH and γ -glutamyl-*S*-methylCys was $53 \pm 10\%$, $37 \pm 9\%$, $30 \pm 11\%$ and $39 \pm 9\%$ (average \pm standard deviation), respectively. The percentage incorporation of ^{34}S in *S*-methylCys was $28 \pm 18\%$. Methanethiol is one of the products of methionine degradation, and may serve as a substrate in the proposed thiol transfer reaction catalyzed by GST. If both methyl transfer and thiol transfer mechanisms exist to produce *S*-methylhGSH, the level of ^{34}S -labeled *S*-methylhGSH would be higher than ^{34}S -labeled hGSH because part of isotope labeled *S*-methylhGSH come from ^{34}S -methanethiol.

To trace the fate of the thiol group donor, methanethiol, seeds were incubated with ^{13}C -sodium thiomethoxide and processed for HRMS analysis. Three metabolites in this pathway were found to contain ^{13}C namely SMC, γ -glutamyl-*S*-methylCys and *S*-methylhGSH with an incorporated percentage of $8 \pm 10\%$, $5 \pm 1\%$ and $2 \pm 2\%$, respectively (Figure 3.2).

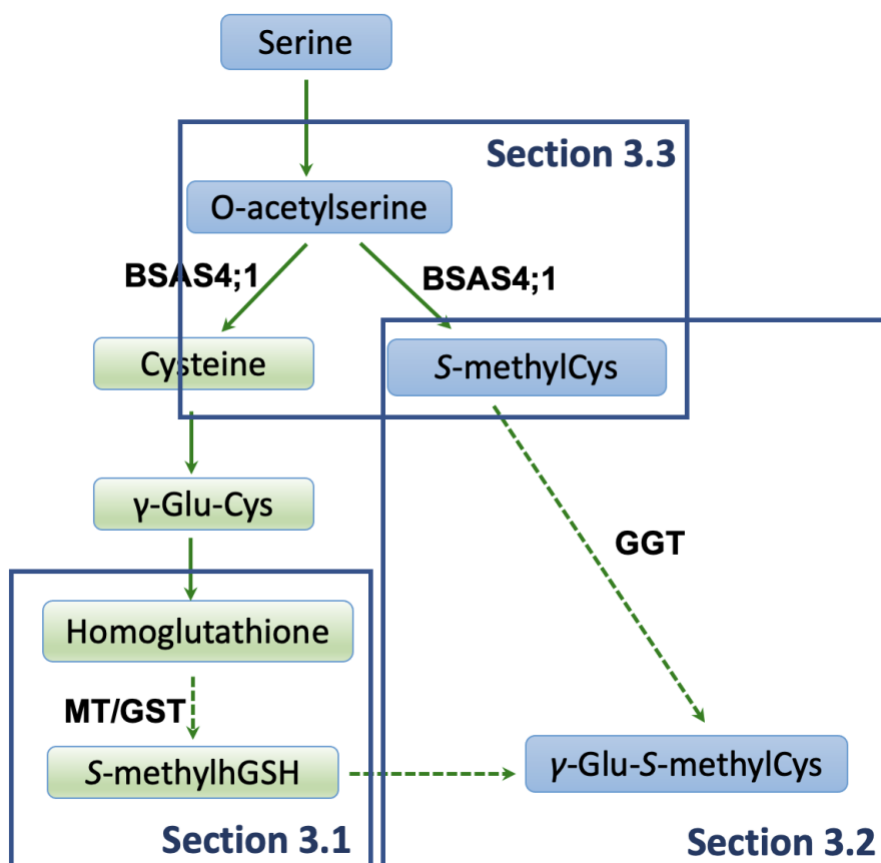


Figure 3.1: The study of non-protein sulphur amino acid biosynthetic pathway corresponding to sections in this thesis.

Solid lines in this simplified scheme indicate sulphur metabolism reported in other studies; while dashed lines indicate putative reactions for metabolite synthesis (Joshi et al., 2019a). Section 3.1 studies the mechanism of *S*-methylhGSH biosynthesis; Section 3.2 studies the potential enzyme GGT involved in γ -Glu-*S*-methylCys biosynthesis; Section 3.3 studies a potential inhibitor in *S*-methylCys.

Glu: glutamyl; Cys: cysteine; BSAS: β -substituted alanine synthase; MT: methyltransferase; GST: glutathione-*S*-transferase; hGSH: homogluthathione; GGT: γ -glutamyl transpeptidase.

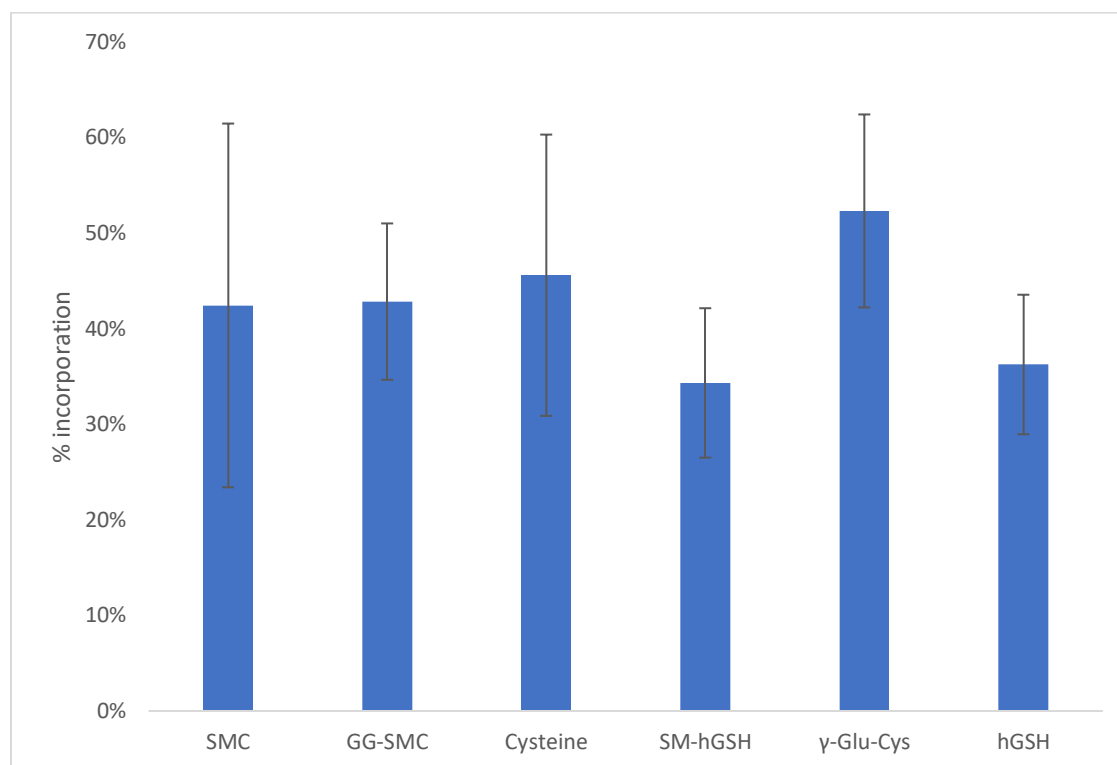


Figure 3.2a: Uptake and incorporation of ^{34}S labeled methionine in developing seeds.

Seeds were cultivated in the presence of 8 mM ^{34}S -methionine. Incorporation of ^{34}S isotope in different *S*-metabolites is presented as % incorporation. The mean percentage incorporation of ^{34}S in *S*-methylCys, γ -glutamyl-*S*-methylCys, cysteine, *S*-methylhGSH, γ -Glu-Cys and hGSH was $42 \pm 19\%$, $43 \pm 8\%$, $46 \pm 15\%$, $34 \pm 8\%$, $52 \pm 10\%$, $36 \pm 7\%$ (average \pm standard deviation), respectively. $n = 6$ except for cysteine data, $n = 3$.

γ -Glu-Cys: γ -glutamylcysteine; hGSH: homoglutathione; SM-hGSH: *S*-methylhomoglutathione; GG-SMC: γ -glutamyl-*S*-methylcysteine; SMC: *S*-methylCys.

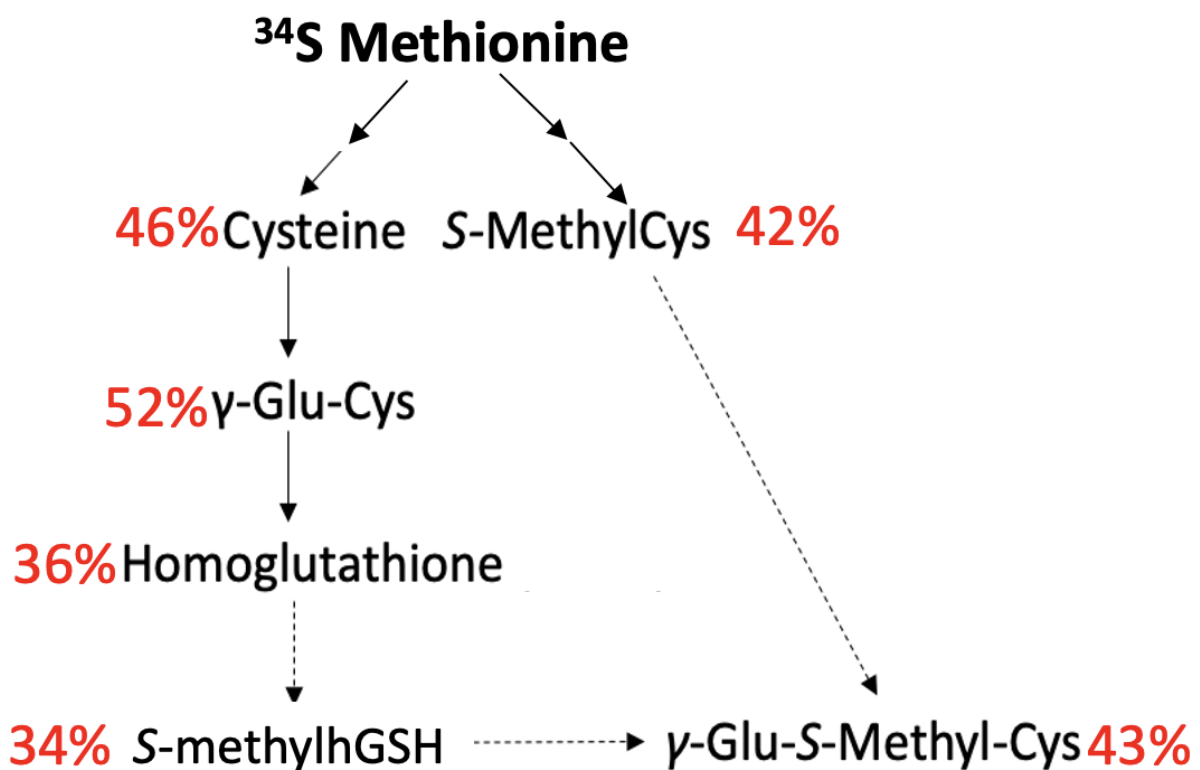


Figure 3.2b: Alternative scheme presenting ^{34}S labeled methionine incorporated into S-containing metabolites in the non-protein sulphur amino acid biosynthetic pathway.

Seeds were cultivated in the presence of 8 mM ^{34}S -methionine. The mean incorporation percentage of ^{34}S isotope in different S-metabolites in this pathway is presented in red.

Glu: glutamyl; Cys: cysteine; hGSH: homoglutathione.

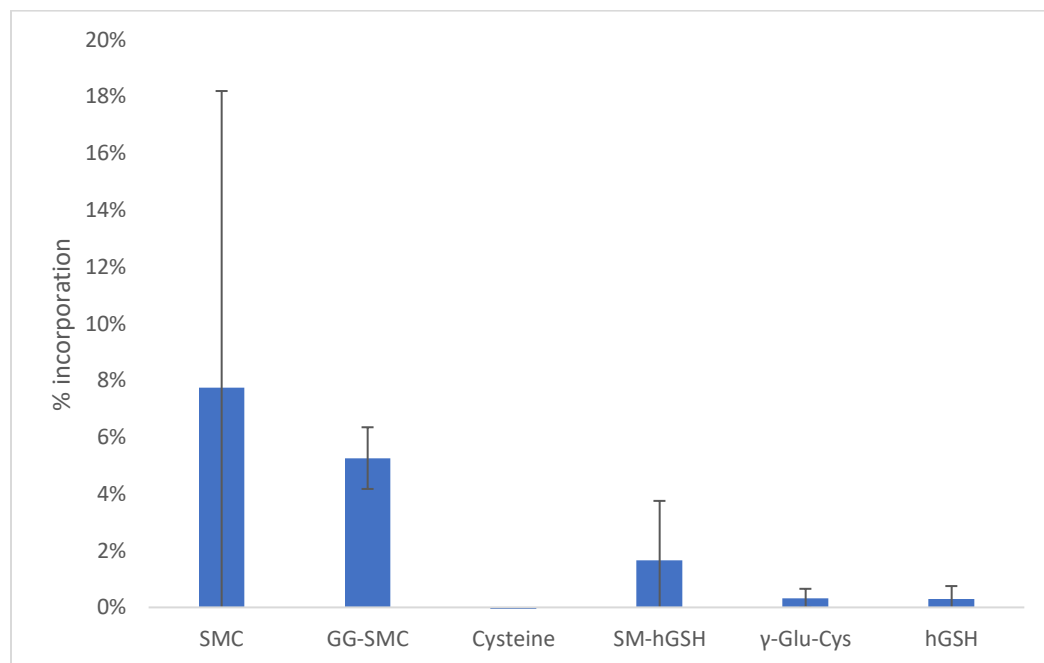


Figure 3.3a: Uptake and incorporation of ^{13}C labeled sodium thiomethoxide in developing seeds.

Seeds were cultivated in the presence of 8 mM ^{13}C -sodium thiomethoxide. Incorporation of ^{13}C isotope in different *S*-metabolites is presented as % incorporation. The mean percentage incorporation of ^{13}C in *S*-methylCys, γ -glutamyl-*S*-methylCys and *S*-methylhGSH was $8 \pm 10\%$, $5 \pm 1\%$ and $2 \pm 2\%$ (average \pm standard deviation), respectively. There was no ^{13}C detected in cysteine, hGSH or γ -Glu-Cys. $n = 14$ except for cysteine data, $n = 8$.

γ -Glu-Cys: γ -glutamylcysteine; hGSH: homoglutathione; SM-hGSH: *S*-methylhomoglutathione; GG-SMC: γ -glutamyl-*S*-methylcysteine; SMC: *S*-methylCys.

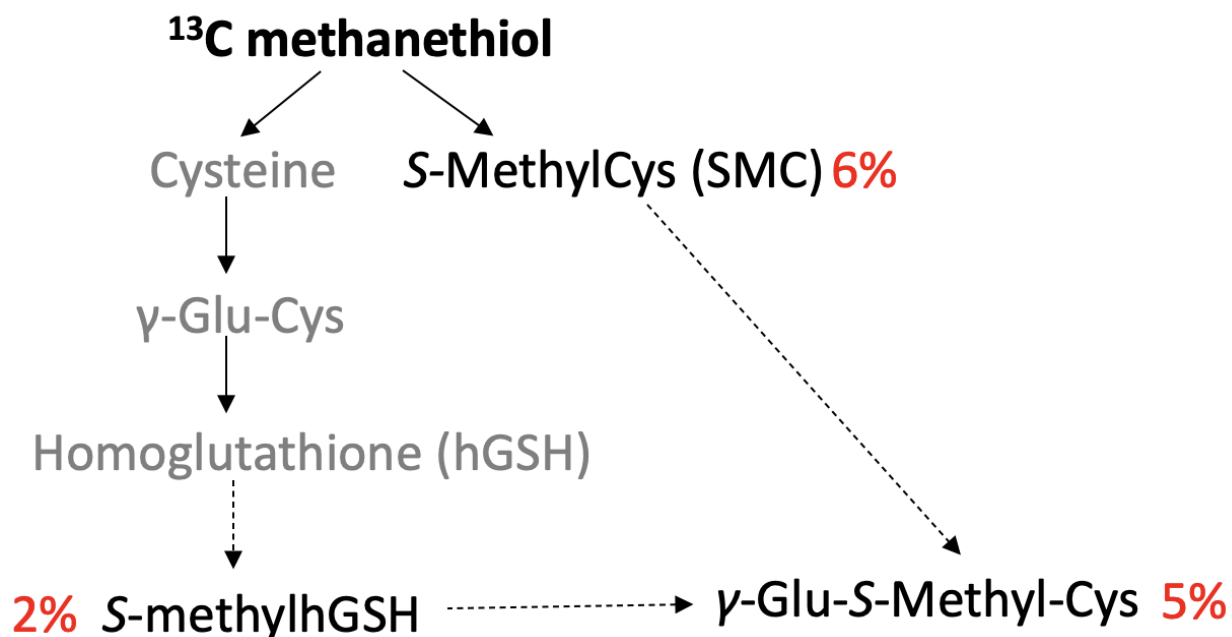


Figure 3.3b: Alternative scheme presenting ^{13}C labeled sodium thiomethoxide incorporated into S-containing metabolites in the non-protein sulphur amino acid biosynthetic pathway.

Seeds were cultivated in the presence of 8 mM ^{13}C -sodium thiomethoxide. The mean incorporation percentage of ^{13}C isotope in different S-metabolites in this pathway is presented in red. S-Metabolites shown in grey indicates no incorporation or low or negligible incorporation.

Glu: glutamyl; Cys: cysteine; hGSH: homoglutathione.

3.1.2 Enzyme assay for S-methylhomogluthathione synthesis

3.1.2.1 Candidate genes for S-methylhomogluthathione synthesis

Based on the expression profiles (Appendix A) of methyltransferase (MT) and glutathione-S-transferase (GST) in RNA-Seq based gene expression atlas, one MT gene and two GST genes were selected as candidate genes (Table 3.1) (O'Rourke et al., 2014). Selected genes were annotated as OMT, GST-u17 and GST-u19. These genes have relatively high expression in seeds and specificity of seed expression. According to WOLF pSORT prediction (<http://www.genscript.com/wolf-psort.html>) (Horton et al., 2007), OMT and GST-u19 are localized in cytosol, and GST-u17 is localized in the chloroplast and nucleus. Based on the predicted result from ChloroP (<http://www.cbs.dtu.dk/services/ChloroP/>), none of these genes encode a chloroplast transit peptide (cTP). Candidate genes OMT, GST-u17 and GST-u19 were cloned and expressed in *E. coli* as His-tagged recombinant proteins and used in enzyme assays. Enzyme assay samples were analyzed by HPLC, no activity was detected. Several MT genes were previously tested in the enzyme assay by a former student, Swati Sood, no activity was detected (Table 3.2). For other MT genes containing cTP in Table 3.2, corresponding recombinant proteins were expressed in a mature form without cTP.

Table 3.1: Molecular and genetic characteristics of methyltransferase (MT) and glutathione-S-transferase (GST) candidate genes

Gene name	Accession number	Gene description	Gene location	Coding sequence (bp)	Predicted protein molecular weight (kDa)	Subcellular localization *
OMT	Phvul.008G 250600	O- methyltransferase	Chr08:5995444 7..59955800	1074	40.23	Cytosol
GST-u17	Phvul.003G 071300	Glutathione-S- transferase u17 related	Chr03:1097270 9..10973987	675	25.47	Nucleus/chloroplast
GST-u19	Phvul.003G 123300	Glutathione-S- transferase u19 related	Chr03:3085374 7..30856141	657	25.18	Cytosol

*Subcellular localization of isoforms was predicted using WoLF PSORT a protein subcellular localization prediction tool. kDa: kilodalton

Table 3.2: Other methyltransferase genes tested in enzyme assays

Gene description	Accession number	Gene location	Subcellular localization*	Presence of cTP**
Carboxymethyltransferase	Phvul.006G048600	Chr06:15356659..15360717	Cytosol	-
Methyltransferase PMT6-related	Phvul.007G248100	Chr07:37098955..37107864	Cytosol	Yes
O-methyltransferase	Phvul.008G247600	Chr08:59667944..59669399	Cytosol	-
Methyltransferase	Phvul.009G015500	Chr09:2532567..2534441	Cytosol/vacuoles	Yes
Caffeate O-methyltransferase	Phvul.009G259200	Chr09:37912481..37914486	Cytosol	-

*Subcellular localization of isoforms was predicted using WoLF PSORT a protein subcellular localization prediction tool. kDa: kilodalton

**Presence of chloroplast transit peptide (cTP) was predicted using ChloroP a cTP prediction tool.

3.1.2.2 Recombinant protein purification and enzyme assays

Candidate genes presented in Table 3.1 were cloned into bacterial expression vectors pQE30 and expressed in *E. coli*. Recombinant protein purification was performed using HiTrap His-tag column on ÄKTA pure system. Purified proteins were analyzed on a 12% gel by SDS-PAGE before using in enzyme assays. Possible methyl donors in this reaction are *S*-adenosylmethionine (SAM), *S*-methylmethionine (SMM), methyltetrahydrofolate and trimethylglycine. With MT, substrates in the enzyme assay were homoglutathione and one of the possible methyl donors. Substrates were homoglutathione and sodium thiomethoxide when GST was added to catalyze the reaction. Seed extracts were also used as a source of enzyme in enzyme assays. Based on the HPLC results, there was no transformation of the substrates into the reaction product with any of the recombinant proteins from the candidate gene list or seed extract (data not shown).

3.2 Study of the biosynthesis of γ -Glu-S-methylCys

3.2.1 γ -Glutamyl transpeptidase candidate genes for γ -Glu-S-methylCys biosynthesis

Based on an annotation search in *P. vulgaris v2.1* available in Phytozome, two γ -glutamyl transpeptidase (GGT) genes were found. They are *Phvul.001G249200* (*PvGGT1*) and *Phvul.004G173700* (*PvGGT4*). *PvGGT1* has two alternative transcripts, which are *Phvul.001G249200.1* (*PvGGT1.1*) and *Phvul.001G249200.2* (*PvGGT1.2*). *PvGGT4* has five alternative transcripts. They are *Phvul.004G173700.1* - *Phvul.004G173700.5* (*PvGGT4.1* - *PvGGT4.5*).

The expression profiles of *PvGGT1* and *PvGGT4* from the RNA-Seq based gene expression atlas of the common bean are presented in Appendix B (O'Rourke et al., 2014). From the expression profile, *PvGGT4* has a higher expression in seeds as compared to *PvGGT1*. Both GGT genes are predominantly expressed at the early stages of seed development as shown at Appendix B, in which expressions at PvSH stage are higher than PvS1 and PvS2.

3.2.2 Biochemical assay with γ -GPNA

To determine the activity of GGT enzyme, a biochemical assay using γ -glutamyl-*p*-nitroanilide (γ -GPNA) and glycylglycine as substrates was performed. Crude protein extracts from developing seeds were precipitated by 30% and 70% ammonium sulphate and tested in γ -GPNA assay. The highest GGT activity was observed in the 30% ammonium sulphate precipitation compared to crude extract and protein after 70% ammonium sulphate precipitation. Therefore, protein collected after 30% precipitation was further purified by HiTrap Phenyl HP column. After hydrophobic interaction chromatography, resulting fractions were pooled based on the UV chromatogram (Figure 3.3). To evaluate the level of GGT activity in three main fractions (frac #1, frac #2, frac #3), γ -GPNA assay was performed. The GGT activity of fraction #1, #2, #3 is presented in Figure 3.4. Fraction #3 showed highest GGT activity, and it was used in following enzyme assay.

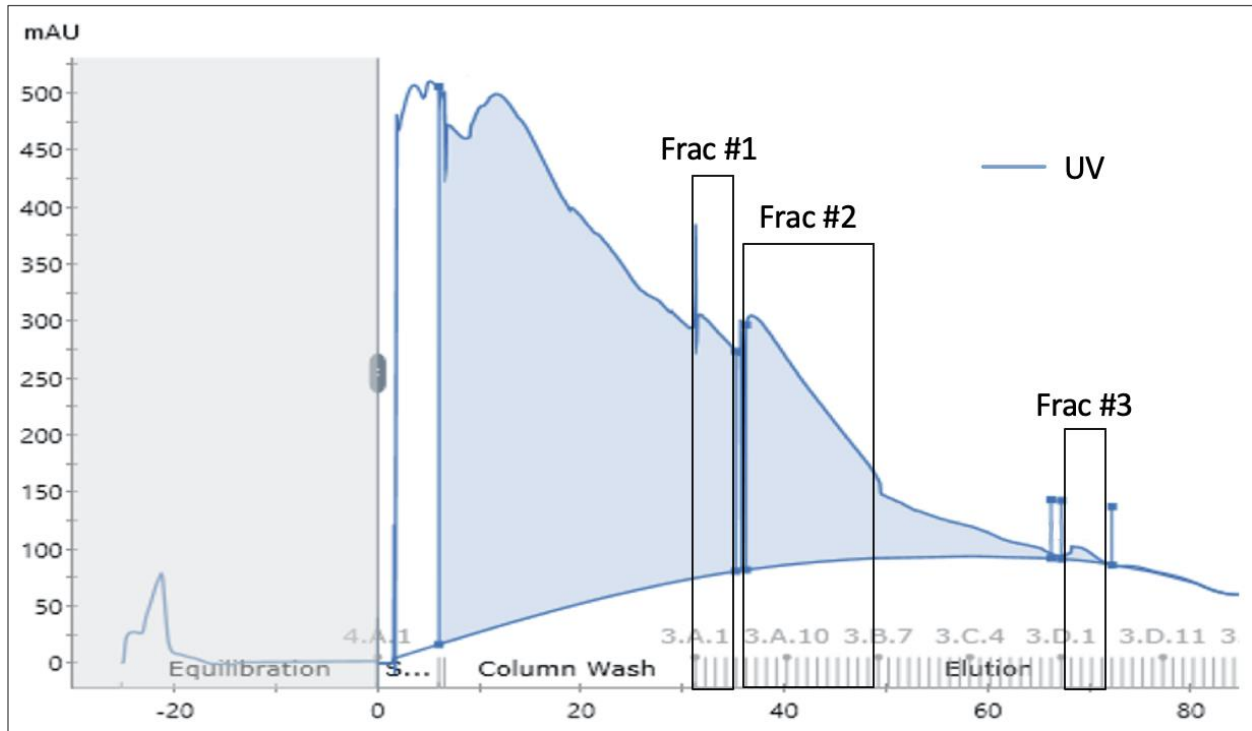


Figure 3.4: Hydrophobic interaction chromatography of proteins from developing seeds.

Fractions were pooled into three main fractions: frac #1, frac #2 and frac #3 based on peaks in UV (A280) chromatogram. These fractions were then used in γ -GPNA assay to test GGT activity.

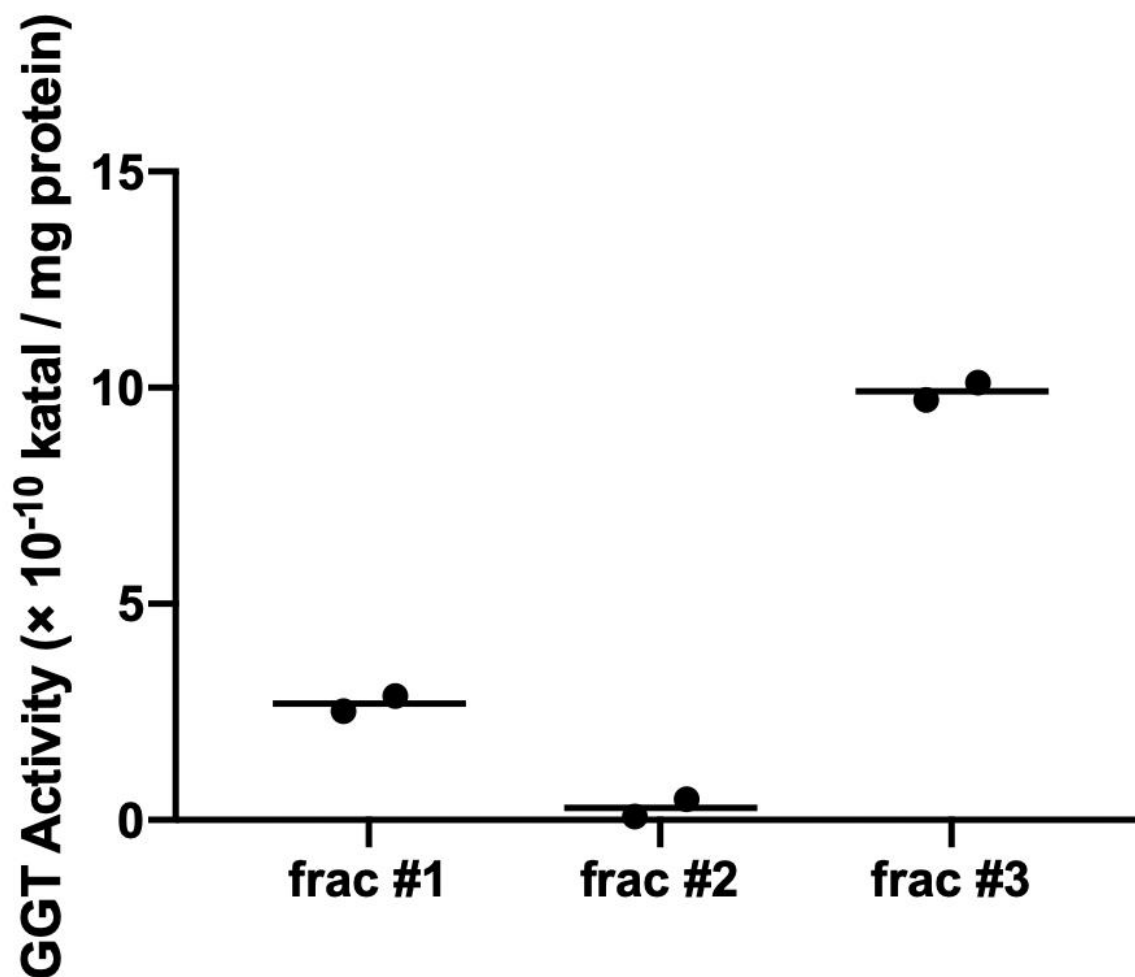


Figure 3.5: GGT activity in different pooled fractions of seed proteins after hydrophobic interaction chromatography.

The GGT activity of different fractions was determined by the transformation of γ -GPNA to PNA during 30 min reaction time. Samples were prepared in duplicate. Dots represent individual data point, and lines represent mean value. The mean of GGT activity of fractions #1, #2, #3 for p-nitroaniline (PNA) production was 2.69×10^{-10} katal mg^{-1} , 0.28×10^{-10} katal mg^{-1} and 9.92×10^{-10} katal mg^{-1} , respectively. $n = 2$.

Katal = $\text{mol}^{-1} \text{sec}^{-1}$.

3.2.3 Enzyme assay with seed extract

After precipitating seed extract by ammonium sulfate and further purifying by HiTrap Phenyl HP column, fraction #3 from seed extract was used in enzyme assay. Substrates in the enzyme assay were homogluthathione (hGSH) and *S*-methylCys (SMC). According to the HPLC results, γ -glutamyl-*S*-methylCys (GG-SMC) was produced in the reaction (Figure 3.5). The GGT activity in seed extract was equal to $9.44 \pm 0.79 \times 10^{-11} \text{ mol}^{-1}\text{sec}^{-1}\text{mg}^{-1}$.

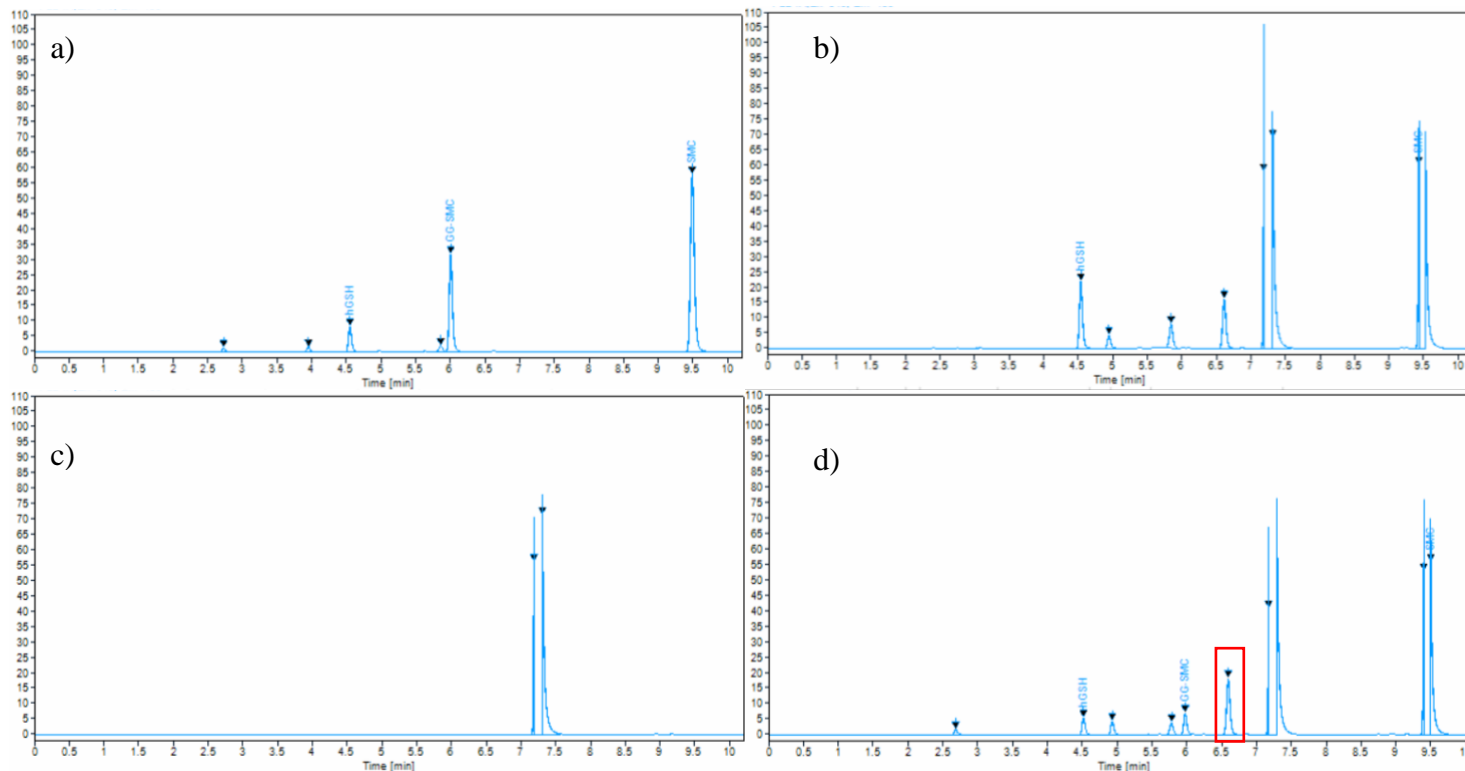


Figure 3.6: HPLC result of enzyme assay with homogluthathione and *S*-methylCys using seed extract as a source of GGT enzyme.

Chromatogram a) shows 100 μ M amino acid standards, including hGSH, γ -Glu-*S*-methylCys and *S*-methylCys; chromatogram b) is reaction control without seed extract; chromatogram c) is control with only 5 μ g seed extract; chromatogram d) is reaction with 5 μ g seed extract and 1 mM substrates. Target product GG-SMC (highlighted in red) was detected in reaction samples shown on chromatogram d. Unit on y-axis is luminescence unit (LU). Peaks at 7.4 min are noise peaks introduced by Tris-HCl buffer while split peaks at 9.5 min indicate large amount of *S*-methylCys was detected.

hGSH: homogluthathione; GG-SMC: γ -glutamyl-*S*-methylcysteine; SMC: *S*-methylcysteine, GGT: γ -glutamyl transpeptidase.

3.2.4 GGT protein purification

For both *PvGGT1* and *PvGGT4*, some alternative transcripts encode shorter forms of the enzymes. Other transcripts encode secreted forms of the enzymes which include a signal peptide, predicted to be localized in the apoplast. Our analysis focused on *PvGGT1.2* and *PvGGT4.2*, likely to encode cytosolic forms of the enzymes.

Mature GGT contains one small (β) and one large (α) subunit, which are generated from the inactive precursor through autocatalytic post-translational processing (Suzuki & Kumagai, 2002). To identify the autocleavage sites in *PvGGT1* and *PvGGT4*, both sequences were aligned with two well-characterized GGT sequences from *E. coli* (*EcGGT*) and *H. pylori* (*HpGGT*) (Castellano et al., 2010) (Appendix C). The predicted protein size of *PvGGT1.2* and *PvGGT4.2* are 51.8 kDa and 61.1 kDa respectively. After autocleavage activity, the size of small and large subunit of *PvGGT1.2* and *PvGGT4.2* were predicted to be 22.2 kDa and 29.6 kDa; and 23.6 kDa and 37.5 kDa, respectively.

The expression of *PvGGT1* and *PvGGT4* was attempted in *E. coli* with pQE30 vector as a N-terminal His-tagged recombinant protein. However, the His-tag mediated purification of GGT proteins was unsuccessful.

3.2.5 Transcripts expression of PvGGT1 and PvGGT4

PvGGT1 has two alternative transcripts, which are *Phvul.001G249200.1* (*PvGGT1.1*) and *Phvul.001G249200.2* (*PvGGT1.2*). *PvGGT4* has five alternative transcripts. They are *Phvul.004G173700.1* - *Phvul.004G173700.5* (*PvGGT4.1* - *PvGGT4.5*).

To investigate the expression level of different transcripts of *PvGGT1* and *PvGGT4*, RT-PCR was performed with total RNA extracted from developing seeds of wild-type BAT93. The total RNA extract was treated with DNase I to prevent DNA contamination.

Primers for *PvGGT1* was designed based on the consensus sequences of *PvGGT1.1* and *PvGGT1.2* (primer 1F and primer 1R) (Appendix D). Two DNA fragments were expected after separating PCR products on a 1% (w/v) agarose gel with sizes of 2.2 kb and 2.9 kb. However, no DNA fragment appeared on the agarose gel (data not shown).

A common forward primer was designed for *PvGGT4* (primer 4CF) based on the consensus transcript sequences of *PvGGT4.1*, *4.2*, *4.4*, *4.5*, and a specific forward primer for *PvGGT4.3* (primer 4.3F). Also, a common reverse primer was designed for *PvGGT4* (primer 4CR) based on the consensus transcript sequences of *PvGGT4.1*, *4.2*, *4.3*, *4.5*, and there was a specific reverse primer for *PvGGT4.4* (primer 4.4R) (Appendix E). DNA fragments were expected on the agarose gel with the combination of primer 4CF and primer 4CR; primer 4CF and primer 4.4R; or primer 4.3F and primer 4CR. However, no DNA sequences were amplified (data not shown).

Therefore, another RT-PCR was conducted using the primers from the coding sequence (CDS) of *PvGGT1* and *PvGGT4*, which are primer-CDS1F and primer-CDS1R; primer-CDS4F and primer-CDS4R (Appendix D and E). Samples using primer-CDS4F and primer-CDS4R showed amplification with a DNA fragment about 1.8 kb (Figure 3.6). There was no DNA fragment on the agarose gel with primer-CDS1F and primer-CDS1R.

In addition to these two trials, there was an attempt of RT-PCR where non-treated DNase I RNA samples were used to synthesize cDNA. There was one smaller DNA fragment (~1.8 kb) and one larger DNA fragment (~4 kb) that appeared on the gel with primer-CDS1F and primer-CDS1R.

Similar results showed on the gel with primer-CDS4F and primer-CDS4R. The bands were purified from agarose gel and sent for Sanger sequencing. Sequencing results revealed that the DNA sequences were amplified correctly with the corresponding primers. Smaller DNA fragments were GGT transcript sequences, while larger fragments were GGT genomic sequences including introns. Based on the sequencing results, a conclusion was that the total RNA extract used in this RT-PCR trial was potentially contaminated with genomic DNA.

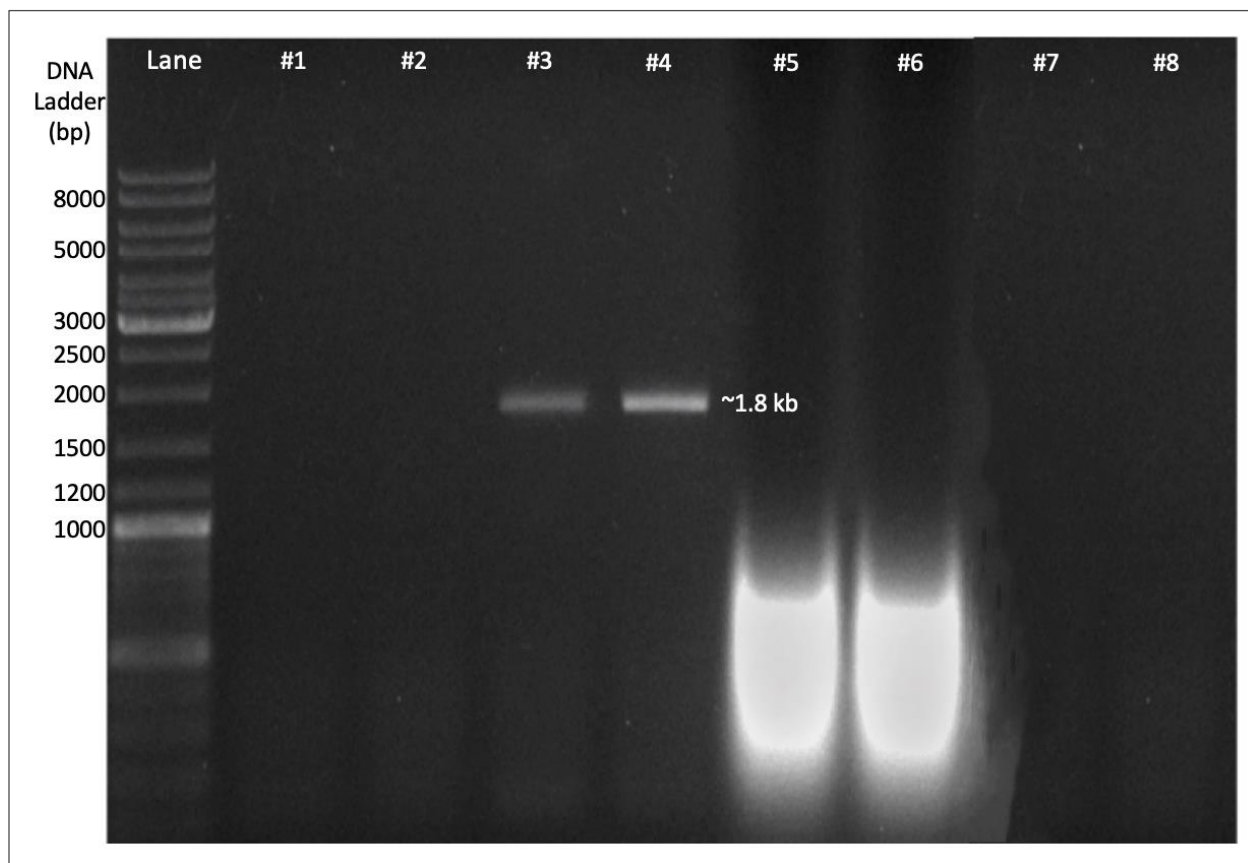


Figure 3.7: Assessment of expression level of different transcripts of *PvGGT1* and *PvGGT4* by RT-PCR.

cDNA synthesized from total RNA extract was used as templates in RT-PCR experiment. Samples were prepared in duplicate. Primers in each sample were as follows: lane #1 and #2 - primer-CDS1F and primer-CDS1R; lane #3 and #4 - primer-CDS4F and primer-CDS4R. Negative controls were: lane #5 included total RNA extract with primer-CDS1F and primer-CDS1R; lane #6 included total RNA extract with primer-CDS4F and primer-CDS4R; lane #7 contained primer-CDS1F and primer-CDS1R only; lane #8 contained cDNA only.

3.2.6 Subcellular localization

PvGGT1.2 and PvGGT4.2 were also selected for subcellular localization experiments. According to WoLF PSORT subcellular localization prediction, PvGGT1.2 and PvGGT4.2 are localized in endoplasmic reticulum (ER) and cytosol, respectively (Horton et al., 2007). Full length sequences of *PvGGT1.2* and *PvGGT4.2* were translationally fused with reporter gene YFP and expressed transiently in epidermal cells of *N. benthamina* leaves. The distribution of cells can be visible under white LED light in confocal microscope. Overlapping of confocal images under white LED light and yellow fluorescent light indicated PvGGT4.2 is mainly expressed in the cytosol (Figure 3.7). Co-localization of PvGGT1.2 with CFP tagged mitochondrial marker protein and RFP tagged nuclear marker protein indicated that PvGGT1.2 localizes in both mitochondria and nucleus (Figure 3.8a, b). Additionally, when the expression of PvGGT1.2 was observed together with chlorophyll autofluorescence at 680-720 nm emission, it was apparent that PvGGT1.2 was also expressed in chloroplasts (Figure 3.8c).

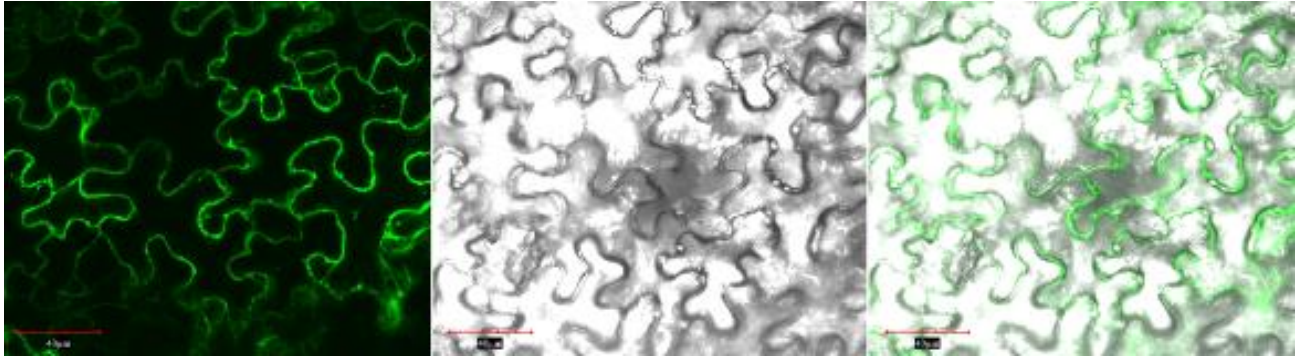


Figure 3.8: Subcellular localization of PvGGT4.2.

Full length *PvGGT4.2* was translationally fused upstream of the reporter gene YFP, transformed into *N. benthamiana* by *A. tumefaciens* mediated transformation and visualized in the epidermal cells of leaves by confocal laser-scanning microscopy. Left panel shows PvGGT4.2 tagged YFP; middle panel shows cells under white LED light; and right panel shows overlapping of PvGGT4.2 and *N. benthamiana* cell images. Scale bar indicates 40 μm .

YFP: yellow fluorescent protein; LED: light-emitting diode.

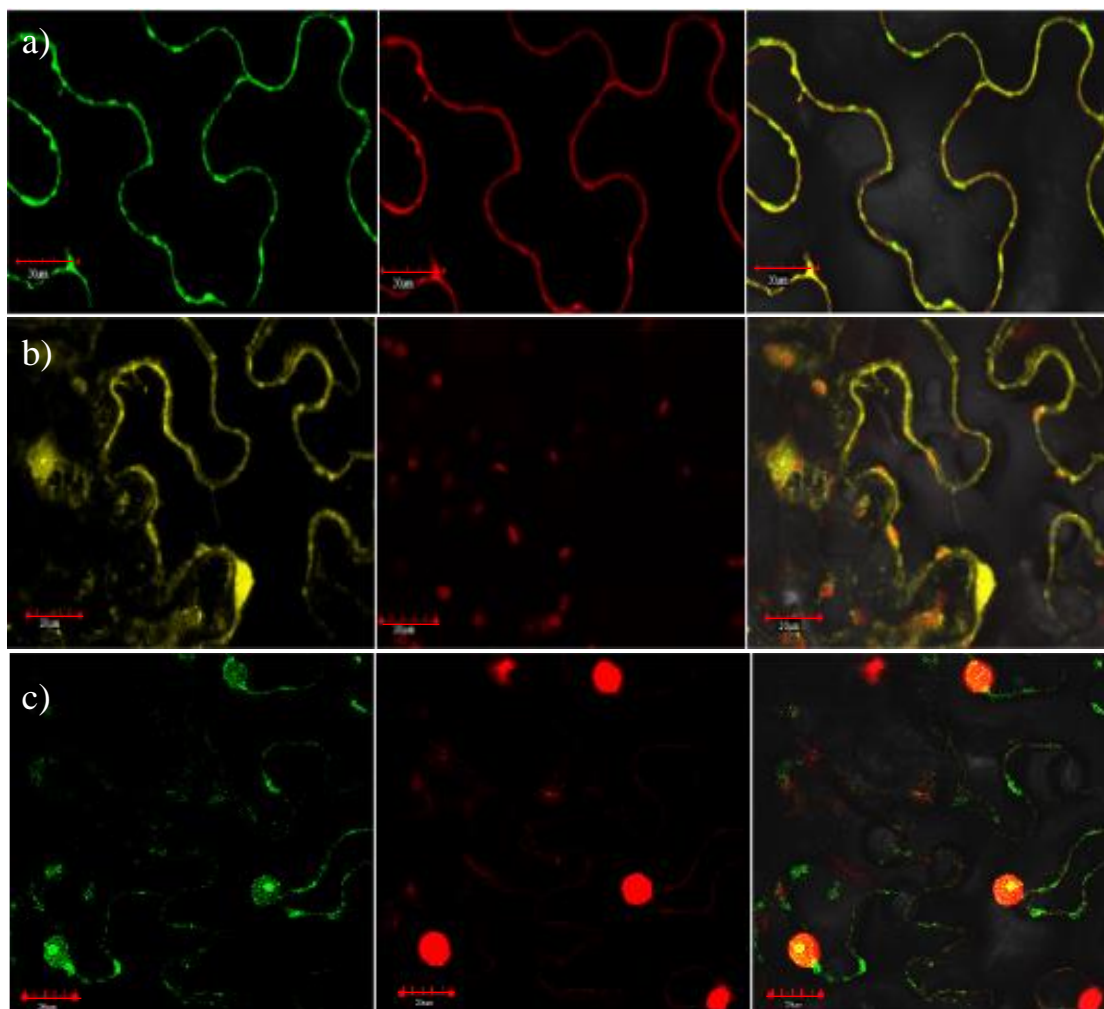


Figure 3.9: Subcellular localization of PvGGT1.2.

Full length *PvGGT1.2* was translationally fused upstream of the reporter gene YFP, transformed into *N. benthamiana* by *A. tumefaciens* mediated transformation and visualized in the epidermal cells of leaves by confocal laser-scanning microscopy. *PvGGT1.2* was co-expressed with different organelle markers. Left panel shows YFP tagged *PvGGT1.2*; middle panel shows the expression of organelle markers or chloroplast under autofluorescence; and right panel shows overlapping of *PvGGT1.2* and organelles. a) and b) show co-localization of *PvGGT1.2* with CFP tagged mitochondrial marker and RFP tagged nuclear marker, respectively. In c), the expression of *PvGGT1.2* was compared and overlapped with chloroplast under autofluorescence. Scale bar indicates 20 μm .

YFP: yellow fluorescent protein; CFP: cyan fluorescent protein; RFP: red fluorescent protein.

3.3 Characterization of benzoic acid as an inhibitor of PvBSAS4;1

3.3.1 Biochemical assay for benzoic acid inhibition

3.3.1.1 Determination of optimal benzoic acid concentration for inhibition

A collaborating laboratory reported crystallographic evidence of benzoate binding in the active site of PvBSAS4;1, which suggests benzoic acid can act as an inhibitor of the enzyme (Milosz Ruszkowski and Mariusz Jaskolski, personal communication).

Initially, a range of benzoic acid concentration between 10 – 2000 μ M was used in enzymatic assay with *O*-acetylserine (OAS) and sodium sulfide as substrates. The production of cysteine was determined with a plate reader using the acid ninhydrin method described by Gaitonde (1976). Figure 3.9 shows the activity of PvBSAS4;1 with varying benzoic acid concentrations. With the increase of benzoic acid concentration, the activity of PvBSAS4;1 decreased. A plateau was observed when benzoic acid concentration was larger than 1.2 mM, the inhibitory effect remained the same with increasing inhibitor concentration. The IC_{50} value of the inhibitor was equal to 0.64 mM.

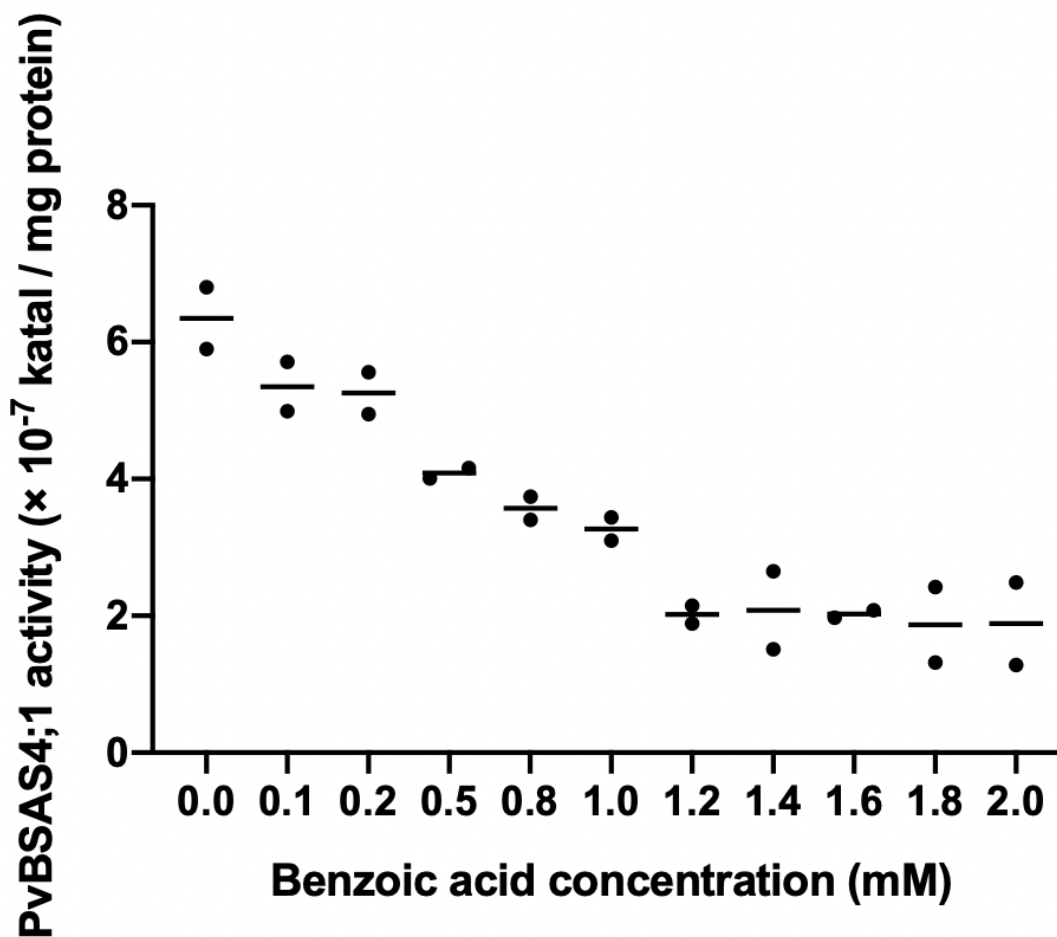


Figure 3.10: Inhibition of PvBSAS4;1 by benzoic acid.

PvBSAS4;1 activity is presented in katal (mol cysteine produced per second) per mg protein. Samples were prepared in duplicate. Dots represent individual data points, and lines represent mean value. The concentration range of benzoic acid in this inhibitory assay was 0 – 2 mM and IC_{50} value was equal to 0.64 ± 0.20 mM (mean \pm standard deviation). $n = 2$.

3.3.1.2 Kinetic studies of benzoic acid

Lineweaver-Burk plot was used to determine the type of inhibition of PvBSAS4;1 by benzoic acid with the reciprocal of the OAS concentration on the x-axis and the reciprocal of reaction rate (in katal per mg) on the y-axis. The V_{max} of the reaction is the intersection of the trendlines of different inhibitor concentrations on the y-axis. The V_{max} remained the same when the inhibitor concentration changed, which indicates that benzoic acid is a competitive inhibitor (Figure 3.10).

A Dixon plot was used to calculate the inhibitor constant (K_i) by varying inhibitor and substrate concentration at the same time. In the Dixon plot, the inhibitor concentration on the x-axis is plotted against the reciprocal of reaction rate in katal per mg. The K_i is the intersection of the trendlines of different substrate concentrations, which is equal to 0.05 mM (Figure 3.11).

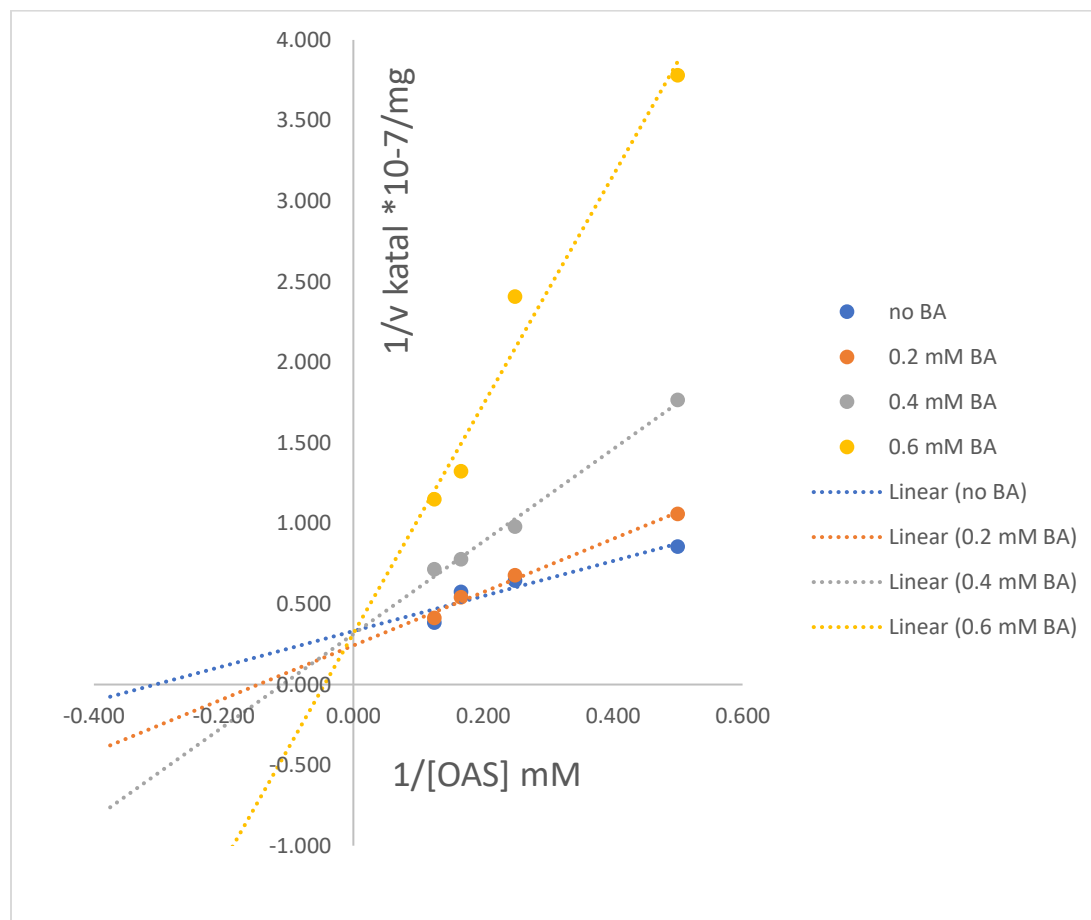


Figure 3.11: Lineweaver-Burk plot for PvBSAS4;1 with a series of OAS and benzoic acid concentrations.

A series concentration of OAS (2 - 8 mM) and benzoic acid (0 - 0.6 mM) were used in the kinetic assay to determine the type of inhibition of PvBSAS4;1 by benzoic acid. The intersection on the y-axis indicates V_{max} of the reaction is not affected by different inhibitor concentrations.

OAS: *O*-acetylserine; BA: benzoic acid.

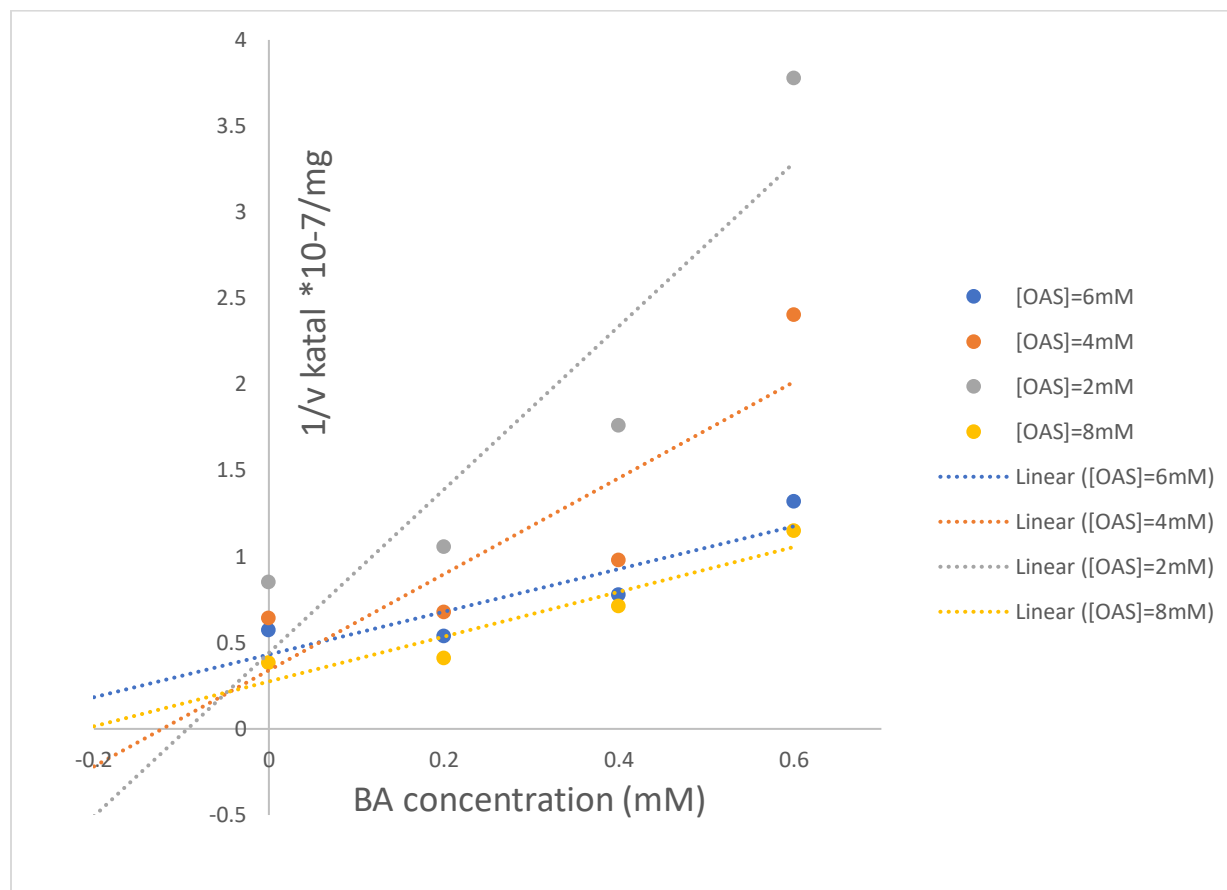


Figure 3.12: Dixon plot with a series of benzoic acid and OAS concentrations.

A series concentration of OAS (2 - 8 mM) and benzoic acid (0 - 0.6 mM) were used in the kinetic assay. The Dixon plot can be used to determine the inhibitor constant (K_i), which is the intersection of the trendlines of different OAS concentrations. K_i is equal to 0.05 mM in this experiment.

OAS: *O*-acetylserine; BA: benzoic acid.

3.3.1.3 Inhibitory effect of other molecules similar to benzoic acid on PvBSAS4;1

Salicylic acid, tyrosine and phenylalanine have similar chemical structures as benzoic acid, and they were used as inhibitor candidates in enzymatic assays. Salicylic acid was an inhibitor of PvBSAS4;1 while tyrosine and phenylalanine did not have any inhibitory effect on the enzyme. Figure 3.12 shows the result of biochemical assay with salicylic acid. The activity of PvBSAS4;1 decreased with the increase of salicylic acid concentration. The IC_{50} value of salicylic acid was equal to 0.61 mM.

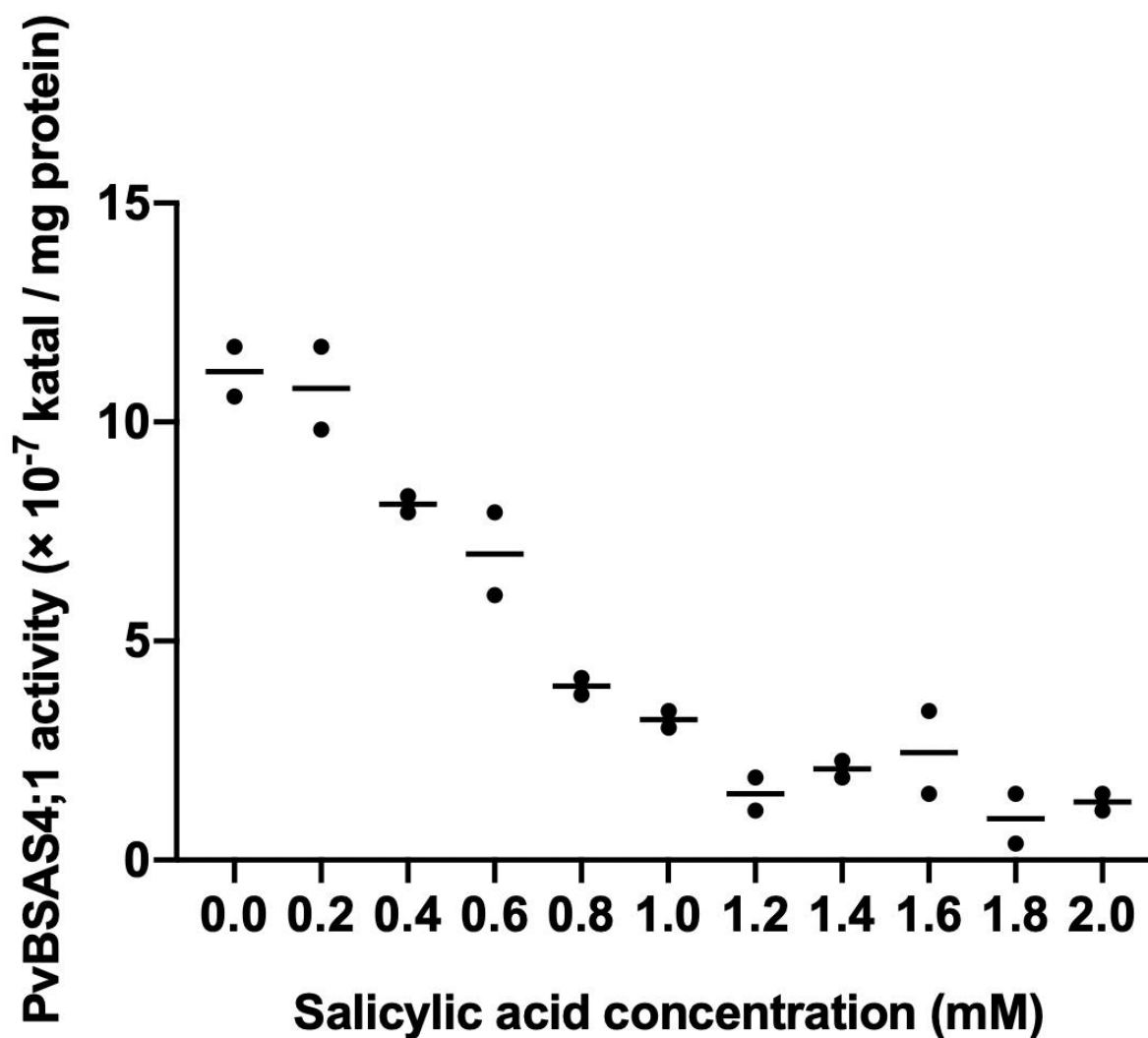


Figure 3.13: Inhibition of PvBSAS4;1 by salicylic acid.

PvBSAS4;1 activity is presented in katal (mol cysteine produced per second) per mg protein. Samples were prepared in duplicate. Dots represent individual data points, and lines represent mean value. The concentration range of salicylic acid in this inhibitory assay was 0 – 2 mM, and IC_{50} value was equal to 0.62 ± 0.10 mM (mean \pm standard deviation). $n = 2$.

3.3.2 *In-vivo* assay with ^{13}C ^{15}N -labelled serine

3.3.2.1 *In-vivo* assay with benzoic acid

Besides enzymatic assay, benzoic acid was added to growth media with ^{13}C ^{15}N -labeled serine to study the *in vivo* effect of this PvBSAS4;1 inhibitor. Based on the appearance of seeds after 48 h incubation with a range of benzoic acid concentration between 0 – 1.2 mM with 0.2 mM interval, all cotyledons were healthy and had a consistent weight increase within this range. Thus, 1.2 mM benzoic acid was chosen to use in the *in-vivo* assay for better observing the inhibitory effect. Samples were analyzed by LC-MS, and each sample included six cotyledons. Based on the result from MS analysis, the percentage incorporation of most downstream metabolites in the biosynthetic pathway of non-protein amino acid decreased by about half (Figure 3.13). These metabolites include cysteine, γ -Glu-Cys, hGSH, *S*-methylhGSH and γ -glutamyl-*S*-methylCys. Among these compounds, the percentage incorporation of γ -glutamyl-*S*-methylCys was very low and undetectable in the presence of benzoic acid; while a dramatic decrease in *S*-methylhGSH incorporation was observed.

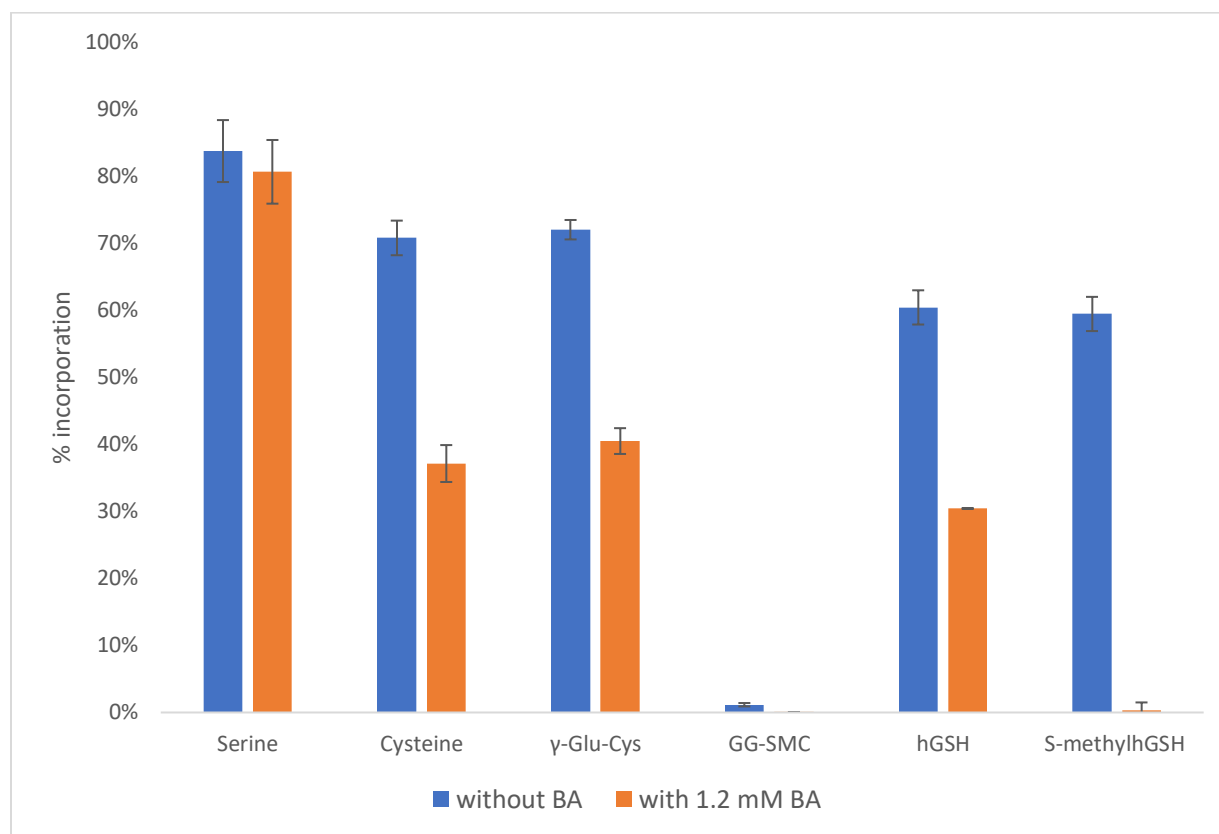


Figure 3.14: Percentage incorporation of labeled compounds in developing seeds following incubation with labeled serine in the presence and absence of benzoic acid.

The treatment groups were supplemented with additional 1.2 mM benzoic acid. Cotyledons were analyzed by HRMS after 48 h incubation. The percentage incorporation of labelled compounds was calculated by determining the ratio of signal intensity of labelled compounds to the sum of labeled and unlabeled signal intensity. In the feeding experiment without adding benzoic acid, the mean percentage incorporation of ^{13}C ^{15}N in serine, cysteine, γ -Glu-Cys, γ -glutamyl-*S*-methylCys, hGSH and *S*-methylhGSH were $84 \pm 5\%$, $71 \pm 3\%$, $72 \pm 1\%$, $1 \pm 0.3\%$, $60 \pm 3\%$, $59 \pm 3\%$, respectively. In the presence of 1.2 mM benzoic acid, the percentage incorporation of ^{13}C ^{15}N in serine, cysteine, γ -Glu-Cys, hGSH and *S*-methylhGSH were $81 \pm 5\%$, $37 \pm 3\%$, $40 \pm 2\%$, $30 \pm 3\%$, 0.1% , $0.3 \pm 1\%$, respectively. $n = 8$.

BA: benzoic acid; γ -Glu-Cys: γ -glutamylcysteine; hGSH: homoglutathione; SM-hGSH: *S*-methylhomoglutathione; GG-SMC: γ -glutamyl-*S*-methylcysteine.

3.3.2.2 *In-vivo* assay with buthionine sulfoximine

Inspired by the incorporation result in the presence of benzoic acid, I was interested to know if one side of the pathway is blocked, what would happen to the other side. Another *in-vivo* assay was performed with buthionine sulfoximine (BSO) in the presence of labeled serine. BSO is a specific inhibitor for the enzyme glutamate-cysteine ligase (GCL), involved in the biosynthesis of γ -Glu-Cys (Hell & Bergmann, 1990). Unexpectedly, there was no decrease of incorporation in any related *S*-metabolites including γ -Glu-Cys (Figure 3.14).

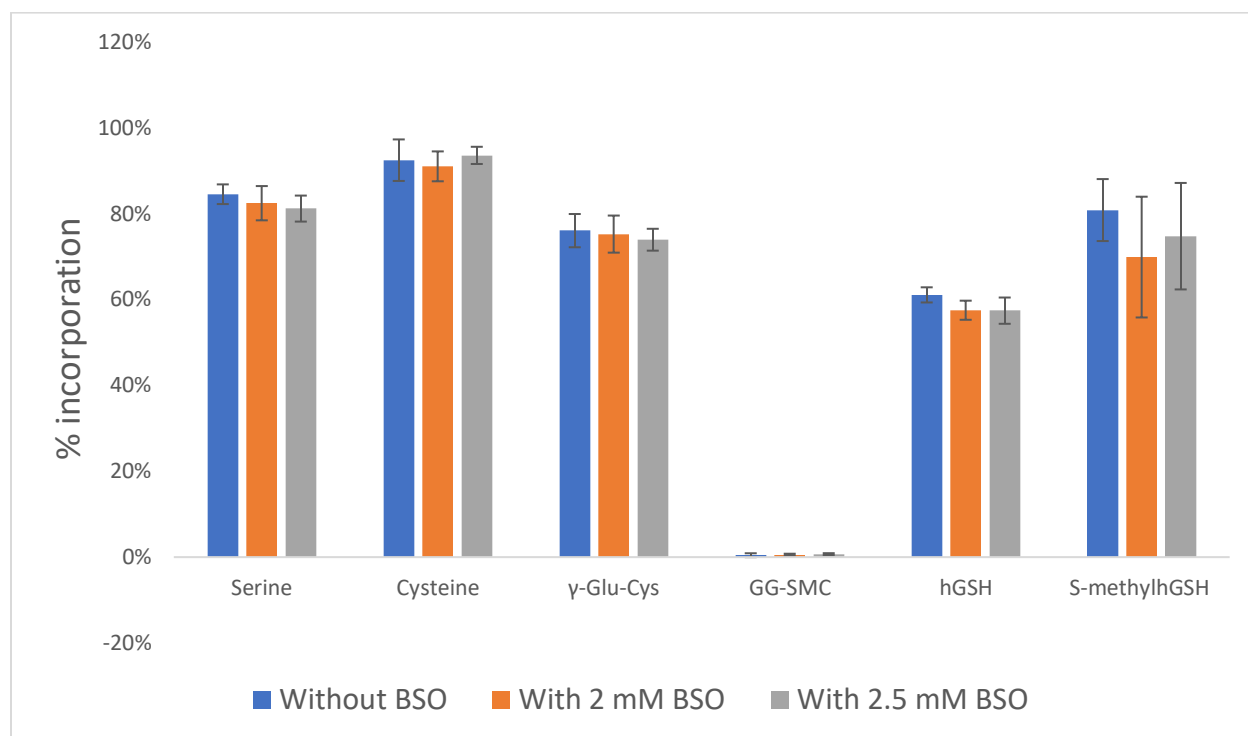


Figure 3.15: Percentage incorporation of labeled compounds in developing seeds following incubation with labeled serine in the presence and absence of BSO.

The treatment groups were supplemented with additional 2 mM or 2.5 mM BSO. Cotyledons were analyzed by HRMS after 48 h incubation. In the feeding experiment without adding BSO, the percentage incorporation of $^{13}\text{C}^{15}\text{N}$ in serine, cysteine, γ -Glu-Cys, γ -glutamyl-*S*-methylCys, hGSH and *S*-methylhGSH were $85 \pm 0.02\%$, $92 \pm 0.04\%$, $76 \pm 0.04\%$, $0.44 \pm 0.01\%$, $61 \pm 0.01\%$, $81 \pm 0.07\%$, respectively. In the presence of 2 mM BSO, the mean percentage incorporation of $^{13}\text{C}^{15}\text{N}$ in serine, cysteine, γ -Glu-Cys, γ -glutamyl-*S*-methylCys, hGSH and *S*-methylhGSH were $82 \pm 0.04\%$, $91 \pm 0.03\%$, $75 \pm 0.04\%$, $0.56 \pm 0.01\%$, $57 \pm 0.02\%$, $70 \pm 0.1\%$, respectively. In the presence of 2.5 mM BSO, the percentage incorporation of $^{13}\text{C}^{15}\text{N}$ in serine, cysteine, γ -Glu-Cys, γ -glutamyl-*S*-methylCys, hGSH and *S*-methylhGSH were $81 \pm 0.03\%$, $94 \pm 0.02\%$, $74 \pm 0.02\%$, $1 \pm 0.01\%$, $57 \pm 0.03\%$, $75 \pm 0.1\%$, respectively. $n = 8$.

BSO: buthionine sulfoximine; γ -Glu-Cys: γ -glutamylcysteine; hGSH: homoglutathione; SM-hGSH: *S*-methylhomoglutathione; GG-SMC: γ -glutamyl-*S*-methylcysteine.

Chapter 4

4 Discussion

4.1 The biosynthesis of *S*-methylhomoglutathione

The primary purpose of this project was to study the biosynthetic pathway of *S*-metabolites in the seed of common bean, including enzymes involved and the mechanisms of the biosynthesis of *S*-methylhGSH. Previous studies suggested that *S*-methylhGSH is a major intermediate leading to the accumulation of the dipeptide of the non-protein amino acid, γ -Glu-*S*-methylCys (Joshi et al., 2019b). In this study, the combination of isotope tracking and high-resolution mass spectrometry (HRMS) methods was used to study the biosynthesis of *S*-methylhGSH in the seed of common bean.

Sulphur is an essential macroelement in biological systems, and protein quality in plants is considered correlated with the amount of essential sulphur amino acids (Sgarbieri & Whitaker, 1982; Leustek et al., 2000). Legumes accumulate homoglutathione as the major storage form of reduced sulphur instead of glutathione (Matamoros et al., 1999). Past isotope incorporation results provided evidence for the synthesis of *S*-methylhGSH in developing seeds of common bean (Joshi et al., 2019a). It also suggested that the biosynthesis of *S*-methylhGSH is likely to take place in plastids (Joshi et al., 2019a).

Müller et al. (2001) showed that Glutathione-*S*-transferase T1 (GSTT1-1) catalyzed the reaction between glutathione and methyl bromide to synthesize *S*-methylglutathione *in-vitro*. One proposed mechanism is an additional methyl group transferred to homoglutathione to produce *S*-methylhGSH. Some possible methyl donors include *S*-adenosylmethionine (SAM) and *S*-methylmethionine (SMM), which are universal methyl donors in methylation reactions in plants. Although betaine (trimethylglycine) serves as a methyl donor in the methionine cycle in mammals, it was also shown to be the precursor for the methylation reaction to produce homostachydrine in *Citrus* (Craig, 2004; Servillo et al., 2012). Additionally, methyltetrahydrofolate provides the

methyl group to homocysteine to synthesize methionine in *E. coli* (Crichton, 2012). Therefore, betaine and methyltetrahydrofolate were also considered as potential methyl donor candidates in this reaction.

It has been reported that methanethiol is a substrate that can replace cyanide to provide the thiol group in *S*-methylCys biosynthesis catalyzed by cyanoalanine β -synthase (CBS) in blue lupine and spinach (Hendrickson & Conn, 1969; Ikegami et al., 1989). A condensation reaction between *O*-acetylserine (OAS) and methanethiol produces *S*-methylCys in common bean. This involves transfer of the thiol group from methanethiol to OAS (Joshi, et al., 2019a). Using the biosynthesis of *S*-methylCys as a guide, another possible mechanism for thiol incorporation into *S*-methylhGSH is the replacement of the thiol group in homoglutathione with methanethiol. Glutathione-*S*-transferases (GSTs) are enzymes that mainly catalyze the conjugation of glutathione involved in detoxification in plants (Shimabukuro et al., 1970). It is also known to catalyze thiol transferase and glutathione peroxidase reactions (Board & Menon, 2013). We proposed that GST catalyzes this thiol transfer reaction between homoglutathione and methanethiol.

Methionine can be converted to methanethiol, β -ketobutyrate and ammonia by methionine- γ -lyase (MGL). The methanethiol produced then serves as a substrate for *S*-methylCys biosynthesis (Joshi et al., 2019a; Joshi & Jander, 2009). This can help explain the $42 \pm 19\%$ ^{34}S isotopic ions recovered in *S*-methylCys. The incorporation of ^{34}S isotope into dipeptide γ -Glu-*S*-methylCys is higher than either *S*-methylCys or *S*-methylhGSH suggesting both metabolites contribute to the synthesis of γ -Glu-*S*-methylCys. This finding is in line with results from a previous study that a similar amount of isotope from serine and cysteine was recovered in γ -Glu-*S*-methylCys (Joshi et al., 2019a). Using ^{34}S -methionine in a feeding experiment to track sulphur movement in the metabolic pathway provides us with insight into the biosynthesis of *S*-methylhGSH. One limitation of this approach was sulfide from methionine catabolism could be utilized everywhere in cells.

In the feeding experiment with ^{34}S -methionine (Figure 3.1), similar recovery of ^{34}S isotope in homoglutathione and *S*-methylhGSH indicates there is no preferential incorporation of ^{34}S into *S*-methylhGSH that would indicate thiol exchange in this biosynthesis. Therefore, the mechanism of *S*-methylhGSH biosynthesis in the seed of common bean is likely to be methyl transfer. However,

trace amount of ^{13}C -labeled *S*-methylhGSH presented in the seed samples treated with ^{13}C -sodium thiomethoxide indicates small amount of thiol group from methanethiol participated in the synthesis of *S*-methylhGSH. In addition, the presence of ^{13}C -labeled *S*-methylCys in agreement with results from a previous isotope tracking experiment confirms that methanethiol was the substrate in the condensation reaction to produce *S*-methylCys (Joshi, et al., 2019a).

The initial breakdown of methionine is catalyzed by amino acid oxidase or transaminase to produce α -ketomethiobutyrate in aminotransferase reactions; then α -ketomethiobutyrate can give rise to branched-chain amino acids (Goyer et al., 2006). The breakdown of branched-chain amino acids into α -keto acids and further to acyl-CoA can serve as a substrate for the synthesis of *S*-containing compounds (Binder & Schuster, 2007). Another methionine catabolism study in *Arabidopsis* indicated that cleavage of methionine can result in the formation of isoleucine and a storage form for methyl group or sulfide (Rébeillé et al., 2006). These could help explain why other metabolites in the pathway also had similar amounts of ^{34}S from methionine as *S*-methylhGSH. The incorporation results give us more information on the non-protein sulphur amino acid biosynthetic pathway; it also provides a guide for future candidate gene search, which should focus on plastidic methyltransferase.

The selection of candidate genes was focused on plastidial/chloroplastic methyltransferases. Unfortunately, the characterization of candidate genes was not successful as none of the candidate gene tested appeared to catalyze the transformation of homogluthathione (hGSH) to *S*-methylhGSH. Our future plan is to identify the methyltransferase gene using an assay with the model substrate methyl bromide (MeBr) to help reveal the methyl donor in this reaction.

4.2 The biosynthesis of γ -Glu-*S*-methylCys

γ -Glu-*S*-methylCys is the dipeptide of the non-protein amino acid *S*-methylCys. The observation that *S*-methylhGSH decreases in parallel with a rapid increase of γ -Glu-*S*-methylCys level in early seed development of common bean suggests that *S*-methylhGSH is converted to γ -Glu-*S*-methylCys and serves as a reservoir for sulphur accumulation (Saboori-Robat et al., 2019). Past studies on kidney bean fruit (*Phaseolus vulgaris* L.) showed that γ -Glu-*S*-methylCys synthesized

from *S*-methylCys with either γ -glutamyl aniline or glutathione was catalyzed by γ -glutamyl transpeptidase (GGT), and that *S*-methylCys is the γ -glutamyl acceptor (Thompson et al., 1964). In garlic, cleavage of the γ -glutamyl moiety from an intermediate *S*-alk(en)yl-L-cysteine sulfoxides in the presence of GGT leads to *S*-alk(en)yl-L-cysteine sulfoxides production (Yoshimoto et al., 2015). Similarly, the removal of γ -glutamyl from hGSH to *S*-methylCys by GGT could lead to the production of γ -Glu-*S*-methylCys.

The GGT protein was successfully purified from tomato and mushroom by using ammonium sulfate precipitation and sepharose column chromatography (Li et al., 2012; Martin et al., 1995). Similar methods were used in this work to purify GGT protein from common bean seeds. It is known that GGT catalyzes the hydrolysis of γ -glutamyl-p-nitroanilide (γ -GPNA); therefore, γ -GPNA assay was used to determine GGT enzyme activity. During the purification process, protein recovered from the pellet after 30% ammonium sulfate precipitation of a crude seed extract showed a higher enzyme activity in the γ -GPNA assay compared to that recovered after 70% ammonium sulfate precipitation. Further in Sepharose column chromatography, the highest GGT activity in one of the fractions was $9.92 \pm 0.28 \times 10^{-10}$ katal mg^{-1} , which is similar as reported in kidney bean fruit (Thompson et al., 1964).

According to the metabolite profiling result from Saboori-Robat et al. (2019), the expression of homoglutathione synthase (hGS) was correlated with the level of the dipeptide γ -Glu-*S*-methylCys. Homoglutathione was proposed to be the γ -glutamyl donor while *S*-methylCys was the γ -glutamyl acceptor in this reaction. γ -Glu-*S*-methylCys was observed in reaction product in HPLC; and the enzyme activity was $9.44 \pm 0.79 \times 10^{-11}$ katal mg^{-1} . The GGT activity is about 10-fold less compared to in γ -GPNA assay. This may be due to GGT enzyme having a higher affinity for γ -GPNA as a reaction substrate compared to homoglutathione. No γ -Glu-*S*-methylCys was detected in seed extracts or substrate samples indicating that there was no contamination in this experiment.

An annotation-based description search of the *P. vulgaris* genome in Phytozome led to the identification of two GGT genes and seven transcripts. They are *PvGGT1* and *PvGGT4*, located on two different chromosomes. Their encoded proteins are predicted to be present in different cellular compartments. Total RNA from wild-type BAT93 was analyzed by RT-PCR using primers

designed from GGT transcript sequences, only transcripts of *PvGGT4* was detected in the product. This finding is consistent with the result from a common bean gene expression atlas (O'Rourke et al., 2014).

γ -Glutamyl peptides were reported to be stored in the cytosol in both garlic and onion (Lancaster et al., 1989; Yoshimoto et al., 2015). In addition, previous isotope tracking experiment in the seed of common bean showed that cells utilized serine to synthesize free *S*-methylCys in cytosol (Joshi et al., 2019a). In our study, transient expression of *PvGGT4* with YFP tag in *N. benthamiana* leaves confirmed *PvGGT4* localization in cytosol in agreement with previous studies. Additionally, my subcellular localization study suggests *PvGGT1* localizes in multiple organelles including mitochondria, chloroplast and nucleus. In conclusion, *PvGGT4* is likely the major player in γ -Glu-*S*-methylCys biosynthesis in common bean.

Later, *PvGGT4* construct was designed, and N-terminus was tagged with His-tag. The autocleavage site was identified to be Thr³⁵², and the molecular masses of large and small subunits were 37.5 kDa and 23.6 kDa, respectively. Unfortunately, expression of *PvGGT* recombinant proteins with *E. coli* as the host resulted in insoluble proteins. In the study of yeast GGT genes, GGT gene was constructed to fuse with *lacZ* and successfully expressed in yeast (Kang et al., 2005). Future attempt in *PvGGT4* recombinant protein expression can use yeast as a host. Besides, Sørensen and Mortensen provided approaches to overcome the insolubility of proteins in *E. coli* by adding expressivity and solubility tags in the construct (Sørensen & Mortensen, 2005).

4.3 Characterization of benzoic acid as an inhibitor

The enzyme *PvBSAS4;1* is the major cysteine synthase (CS) in the seed of common bean (O'Rourke et al., 2014). It catalyzes the condensation reaction between *O*-acetylserine and methanethiol to synthesize *S*-methylCys (Ikegami et al., 1989). The crystal structure of *PvBSAS4;1* from our collaborators showed that benzoate binds to the active site of the enzyme, which suggests benzoic acid might be an inhibitor for *PvBSAS4;1*.

Inhibition of CS has been mostly identified by phenotypic analysis or through natural compounds screening in past studies. One study identified nine natural compounds that can inhibit both classes of CS isotypes in *Entamoeba histolytica* with IC_{50} value of 0.31 – 490 μ M (Mori et al., 2015). Among these nine inhibitors, seven of them share a naphthoquinone moiety and eight of them contain phenol group in their chemical structures (Mori et al., 2015). Another screening study demonstrated 20 compounds that inhibit CS in *Mycobacterium tuberculosis*. Of those, 19 share an aromatic carboxylic acid group (Brunner et al., 2016). Benzoic acid shows antimicrobial activity and functions in the defense response activation in plants (Widhalm & Dudareva, 2015). Benzoic acid and its derivatives showed inhibitory effect on a variety of enzyme families, including demethylase, myeloperoxidase, tyrosinase, *etc.* (Kettle et al., 1995; Liu et al., 2022; Nazir et al., 2020).

To date, inhibition studies for CS were mainly focused on microorganisms, and information about CS in plants is limited. In this study, we demonstrated benzoic acid inhibits the activity of PvBSAS4;1 *in-vitro* with an IC_{50} value of 0.64 mM (Figure 3.13). The IC_{50} value is slightly higher than the maximum IC_{50} value reported for the inhibitors of CS in *E. histolytica* (Mori et al., 2015). Overall, the IC_{50} value is about 10 times higher compared to other studies on CS inhibitors in microbes (Brunner et al., 2016; Kaushik et al., 2021). Analysis of enzyme kinetics revealed that benzoic acid displayed a competitive inhibition in the enzymatic reaction with PvBSAS4;1 (Figure 3.14) with K_i value of 50 μ M. The molecular mechanism of the inhibition is benzoic acid shares a similar shape with the substrates and competes for the active site of PvBSAS4;1 (Carey & Bellelli, 2017). The K_i value of benzoic acid is similar as reported in another study on tyrosinase in mushroom (Nazir et al., 2020). To our knowledge, there have been no experimental data on the influences of benzoic acid on plant CS, which makes it difficult to discuss the affinity of the benzoic acid to PvBSAS4;1.

Besides benzoic acid, other compounds were also selected to test the inhibitory effect on PvBSAS4;1, including salicylic acid, tyrosine and phenylalanine. Among these compounds, only salicylic acid showed inhibitory activity on PvBSAS4;1 with a similar IC_{50} value as benzoic acid. Previous studies showed a common structure among CS inhibitors in different microorganisms

(Brunner et al., 2016; Mori et al., 2015). In this study, only a few phenolic compounds were tested. Given benzoic acid and salicylic acid are both phenolic acids, the critical structure for plant CS inhibitors might be carboxylic acid group attached to a benzene ring. Further inhibition experiments with more benzoic acid derivatives and other CS in plants need to be done to test this hypothesis.

The inhibitory effect of benzoic acid on PvBSAS4;1 was also confirmed in an *in-vivo* experiment with ^{13}C , ^{15}N -serine. In the presence of benzoic acid, the level of incorporation of label into cysteine decreased about half (Figure 3.17). However, benzoic acid also seems to inhibit incorporation of label from ^{13}C , ^{15}N -serine into other downstream metabolites in this pathway, including γ -Glu-Cys, homoglutathione, *S*-methylhGSH and γ -Glu-*S*-methylCys. The isotope incorporation into these compounds decreased by a similar amount as observed for cysteine, with the exception of *S*-methylhGSH, which had no isotope incorporation. An explanation could be inhibiting the biosynthesis of cysteine and *S*-methylCys subsequently affects the synthesis of downstream metabolites. One possible reason for the complete inhibition of serine incorporation into *S*-methylhGSH biosynthesis by benzoic acid is that PvBSAS4;1 may also be involved in the biosynthesis of *S*-methylhGSH. An *in-vivo* experiment using callus tissue showed that levels of cysteine and glutathione both increased in the presence of benzoic acid or salicylic acid (Farghaly et al., 2021). This suggests benzoic acid might not have a consistent effect on CS in different plant species.

Buthionine sulfoximine (BSO) is a specific inhibitor of glutamyl-cysteine ligase (GCL), involved in the first step of glutathione synthesis (Griffith & Meister, 1979). Several studies have demonstrated BSO inhibits the biosynthesis of glutathione in plant cultures *in-vivo* (Alvarez et al., 2011; Scheller et al., 1987). In my study, BSO was used as a potential inhibitor for the biosynthesis of γ -Glu-*S*-methylCys in an *in-vivo* experiment with isotope labeled serine. Similar isotope incorporation levels into γ -Glu-Cys, homoglutathione and other metabolites in different treatment groups indicated that BSO does not have an impact on the biosynthetic pathway of non-protein sulphur amino acids in common bean. Future *in-vitro* experiment with recombinant GCL protein

and BSO might help to understand the lack of inhibitory activity of BSO on homoglutathione biosynthesis in seed of common bean.

Chapter 5

5 Conclusion

5.1 Concluding remarks and future studies

As one of the most consumed food legume crops worldwide, the common bean provides adequate carbohydrate, essential nutrients and valuable protein content. However, the sub-optimal level of essential sulphur amino acids (i.e. methionine and cysteine) limits the protein quality in common bean. The non-protein sulphur amino acid, *S*-methylCys, and its dipeptide γ -Glu-*S*-methylCys accumulate in the seed of common bean as a sulphur storage sink but do not contribute to protein synthesis. The goals of this project were to understand the pathway involved in the biosynthesis of non-protein amino acids in common bean seeds. Our results revealed the major intermediate in this pathway, *S*-methylhGSH, was synthesized in a methyl transfer reaction. This study provided several pieces of evidence using isotopic tracking, enzyme kinetics for the inhibitor role of benzoic acid in *S*-methylCys biosynthesis. Furthermore, results suggested that γ -glutamyl transferase (GGT) catalyzed the biosynthesis of the non-protein sulphur amino acid dipeptide, γ -Glu-*S*-methylCys, in the presence of hGSH and *S*-methylCys.

Future work should focus on identifying candidate genes involved in the pathway of *S*-amino acid derivatives biosynthesis. Understanding sulphur metabolism is crucial to improve our knowledge of plant metabolism.

References

- Altenbach, S. B., Pearson, K. W., Leung, F. W., & Sun, S. M. (1987). Cloning and sequence analysis of a cDNA encoding a Brazil nut protein exceptionally rich in methionine. *Plant Molecular Biology*, 8(3), 239–250.
- Alvarez, S., Galant, A., Jez, J. M., & Hicks, L. M. (2011). Redox-regulatory mechanisms induced by oxidative stress in *Brassica juncea* roots monitored by 2-DE proteomics. *Proteomics*, 11(7), 1346–1350.
- Aragão, F. L., Barros, L. G., Sousa, M. V., Grossi, M. F., Almeida, E. P., Gander, E. S., & Rech, E. L. (1999). Expression of a methionine-rich storage albumin from the Brazil nut (*Bertholletia excelsa*) in transgenic bean plants (*Phaseolus vulgaris* L.). *Genetics and Molecular Biology*, 22(3), 445–449.
- Benjamin T. B. & Theodore S. W. (2003). An intuitive look at the relationship of K_i and IC_{50} : a more general use for the dixon plot. *Journal of Chemical Education*, 90(2), 241.
- Binder, S., Knill, T., & Schuster, J. (2007). Branched-chain amino acid metabolism in higher plants. *Physiologia Plantarum*, 129(1), 68–78.
- Bliss, F. A., & Brown, J. S. (1983). Breeding common bean for improved quantity and quality of seed protein. In J. Janick (Eds.), *Plant Breeding Reviews* (pp. 59-102). Washington, DC: Springer.
- Board, P. G., & Menon, D. (2013). Glutathione transferases, regulators of cellular metabolism and physiology. *Biochimica et Biophysica Acta*, 1830(5), 3267–3288.
- Broughton, W. J., Hernández, G., Blair, M., Beebe, S., Gepts, P., & Vanderleyden, J. (2003). Beans (*Phaseolus* spp.)-model food legumes. *Plant and Soil*, 252, 55-128.
- Brunner, K., Maric, S., Reshma, R. S., Almqvist, H., Seashore, L. B., Gustavsson, A. L., Poyraz, O., Yogeewari, P., Lundback, T., Vallin, M., Sriram, D., Schnell, R., & Schneider, G. (2016). Inhibitors of the Cysteine Synthase CysM with Antibacterial Potency against Dormant *Mycobacterium tuberculosis*. *Journal of Medicinal Chemistry*, 59(14), 6848–6859.
- Brunold, C., & Schiff, J. A. (1976). Studies of sulfate utilization by algae: 15. Enzymes of assimilatory sulfate reduction in euglena and their cellular localization. *Plant Physiol*, 57(3), 430-436.
- Buchner, P., Takahashi, H., & Hawkesford, M. J. (2004). Plant sulphate transporters: Co-ordination of uptake, intracellular and long-distance transport. *Journal of Experimental Botany*, 55(404), 1765–1773.
- Cândido, S. E., Pinto, M. F. S., Pelegrini, P. B., Lima, T. B., Silva, O. N., Pogue, R., Grossi-de-Sá, M. F., & Franco, O. L. (2011). Plant storage proteins with antimicrobial activity: novel insights into plant defense mechanisms. *The FASEB Journal*, 25(10), 3290–3305.

- Carey, J., & Bellelli, A. (2017). Two-Substrate Enzymes and their Inhibitors. In J. Carey & A. Bellelli (Eds.), *Reversible Ligand Binding* (pp. 233–251). Chichester, UK: John Wiley & Sons.
- Castellano, I., Merlino, A., Rossi, M., & Cara, L. F. (2010). Biochemical and structural properties of gamma-glutamyl transpeptidase from *Geobacillus thermodenitrificans*: An enzyme specialized in hydrolase activity. *Biochimie*, 92(5), 464–474.
- Chrispeels, M. J., & Raikhel, N. V. (1991). Lectins, lectin genes, and their role in plant defense. *The Plant Cell*, 3(1), 1–9.
- Craig, S. A. (2004). Betaine in human nutrition. *The American Journal of Clinical Nutrition*, 80(3), 539–549.
- Crichton, R. R. (2012). Nickel and Cobalt. In R. Crichton (Eds), *Biological Inorganic Chemistry* (pp. 297–310). New York, NY: Academic Press.
- Dahl, C., Hell, R., Leustek, T., & Knaff, D. (2008). Introduction to sulphur metabolism in phototrophic organisms. In R. Hell & M. Wirtz (Eds.), *Sulphur Metabolism in Phototrophic Organisms* (pp. 1-14). Netherlands: Springer.
- De Ron, A. M., Papa, R., Bitocchi, E., González, A. M., Debouck, D. G., Brick, M. A., Fourie, D., Marsolais, F., Beaver, J., Geffroy, V., McClean, P., Santalla, M., Lozano, R., Yuste-Lisbona, F. J., & Casquero, P. A. (2015). Common bean. In A. M. De Ron (Eds.), *Grain Legumes* (pp. 1-36). New York, NY: Springer.
- Derbyshire, E. (1976). Isolation of legumin-like protein from *Phaseolus aureus* and *Phaseolus vulgaris*. *Phytochemistry*, 15(3), 411–414.
- FAO. (2013) Dietary protein quality evaluation in human nutrition: report of an FAO expert consultation. *FAO Food and Nutrition*, pp. 92. FAO, Rome.
- FAO. (2014). The statistics division of the FAO. <http://faostat.fao.org/>
- Farghaly, F. A., Salam, H. K., Hamada, A. M., & Radi, A. A. (2021). The role of benzoic acid, gallic acid and salicylic acid in protecting tomato callus cells from excessive boron stress. *Scientia Horticulturae*, 278, 109867.
- Ferla, M. P., & Patrick, W. M. (2014). Bacterial methionine biosynthesis. *Microbiology*, 160, 1571–1584.
- Fjellstedtand, T. A., & Schlesselman, J. J. (1977). A Simple Statistical Method for Use in Kinetic Analysis Based on Lineweaver-Burk Plots. In A. Cooper (Eds.), *Analytical Biochemistry* (pp. 224-238). Orlando, FL: Academic Press.
- Gaitonde, M. (1967). A spectrophotometric method for the direct determination of cysteine in the presence of other naturally occurring amino acids. *Biochemical Journal*, 104(2), 627–633.
- Galvez, A. F., Revilla, M. J., de Lumen, B. O., & Krenz, D. C. (2008). Enhancing the Biosynthesis of Endogenous Methionine-Rich Proteins (MRP) to Improve the Protein Quality of Legumes Via Genetic Engineering. In J. R. Whitaker (Eds.) *Food for Health in the Pacific Rim* (pp. 540–552). Trumbull, Conn: Food & Nutrition Press.

- Giovanelli, J., Mudd, S. H., & Datko, A. H. (1980). Sulphur Amino Acids in Plants. In B. J. Mifflin (Eds.), *Amino Acids and Derivatives* (pp. 453–505). New York, NY: Elsevier.
- Goyer, A., Collakova, E., Shachar-Hill, Y., & Hanson, A. D. (2006). Functional characterization of a methionine -lyase in arabidopsis and its implication in an alternative to the reverse trans-sulphuration pathway. *Plant and Cell Physiology*, *48*(2), 232–242.
- Griffith, O. W., & Meister, A. (1979). Potent and specific inhibition of glutathione synthesis by buthionine sulfoximine (S-n-butyl homocysteine sulfoximine). *Journal of Biological Chemistry*, *254*(16), 7558–7560.
- Harlow, E., & Lane, D. (2006). Bradford Assay. *Cold Spring Harbor Protocols*, *2006*(6), 4644.
- Hell, R., & Bergmann, L. (1990). λ -Glutamylcysteine synthetase in higher plants: catalytic properties and subcellular localization. *Planta*, *180*, 603.
- Hendrickson, H. R., & Conn, E. E. (1969). Cyanide Metabolism in Higher Plants. *Journal of Biological Chemistry*, *244*(10), 2632–2640.
- Horton, P., Park, K. J., Center, H. G., Obayashi, T., & Nakai, K. (2007). WoLF PSORT: protein localization predictor. *Nucleic Acids Research*, *35*(Web Server issue), W585–W587.
- Husain, A., Sato, D., Jeelani, G., Mi-ichi, F., Ali, V., Suematsu, M., Soga, T., & Nozaki, T. (2010). Metabolome analysis revealed increase in s-methylcysteine and phosphatidylisopropanolamine synthesis upon l-cysteine deprivation in the anaerobic protozoan parasite entamoeba histolytica. *Journal of Biological Chemistry*, *285*(50), 39160–39170.
- Ikegami, F., Takayama, K., Kurihara, T., Horiuchi, S., Tajima, C., Shirai, R., & Murakoshi, I. (1989). Purification and properties of β -cyano-l-alanine synthase from *Vicia angustifolia*. *Phytochemistry*, *28*(9), 2285–2291.
- Iwami, K., Yasumoto, K., & Mitsuda, H. (1975). Enzymatic cleavage of cysteine sulfoxide in *Lentinus edodes*. *Agricultural & Biological Chemistry*, *39*(10), 1947–1955.
- Joshi, J. (2017). Deciphering Sulphur Amino Acid Metabolism in Developing Seeds of Common Bean (Doctoral dissertation, The University of Western Ontario, London, CA). Retrieved from <https://ir.lib.uwo.ca/cgi/viewcontent.cgi?article=6681&context=etd>
- Joshi, J., Renaud, J. B., Sumarah, M. W., & Marsolais, F. (2019a). Deciphering S-methylcysteine biosynthesis in common bean by isotopic tracking with mass spectrometry. *Plant Journal*, *100*(1), 176–186.
- Joshi, J., Saboori-Robat, E., Solouki, M., Mohsenpour, M., & Marsolais, F. (2019b). Distribution and possible biosynthetic pathway of non-protein sulphur amino acids in legumes. *Journal of Experimental Botany*, *70* (16), 4115–4121.
- Joshi, V., & Jander, G. (2009). Arabidopsis methionine γ -lyase is regulated according to isoleucine biosynthesis needs but plays a subordinate role to threonine deaminase. *Plant Physiology*, *151*(1), 367–378.

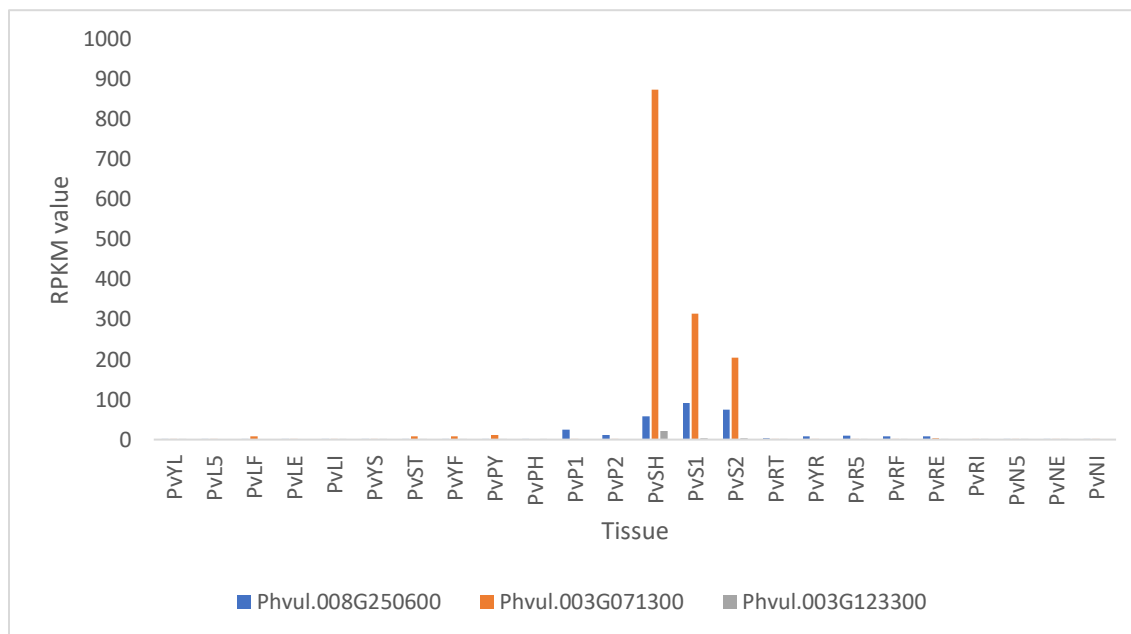
- Kalavacharla, V., Liu, Z., Meyers, B. C., Thimmapuram, J., & Melmaiee, K. (2011). Identification and analysis of common bean (*Phaseolus vulgaris* L.) transcriptomes by massively parallel pyrosequencing. *BMC Plant Biology*, *11*(1), 135.
- Kang, H. J., Kim, B. C., Park, E. H., Ahn, K. S., & Lim, C. J. (2005). The gene encoding γ -glutamyl transpeptidase II in the fission yeast is regulated by oxidative and metabolic stress. *BMB Reports*, *38*(5), 609–618.
- Kaushik, A., Rahisuddin, R., Saini, N., Singh, R. P., Kaur, R., Koul, S., & Kumaran, S. (2021). Molecular mechanism of selective substrate engagement and inhibitor disengagement of cysteine synthase. *Journal of Biological Chemistry*, *296*, 100041.
- Kettle, A. J., Gedye, C. A., Hampton, M. B., & Winterbourn, C. C. (1995). Inhibition of myeloperoxidase by benzoic acid hydrazides. *Biochemical Journal*, *308*(2), 559–563.
- Krishnan, H. B. (2000). Biochemistry and Molecular Biology of Soybean Seed Storage Proteins. *Journal of New Seeds*, *2*(3), 1–25.
- Krueger, R. J., & Siegel, L. M. (1982). Evidence for siroheme-Fe₄S₄ interaction in spinach ferredoxin-sulfite. *Biochemistry*, *21*(12), 2905-2909.
- Lancaster, J. E., Reynolds, P. H. S., Shaw, M. L., Dommissie, E. M., & Munro, J. (1989). Intracellular localization of the biosynthetic pathway to flavour precursors in onion. *Phytochemistry*, *28*(2), 461–464.
- Leustek, T., Martin, M. N., Bick, J. A., & Davies, J. P. (2000). Pathways and regulation of sulphur metabolism revealed through molecular and genetic studies. *Annual Review of Plant Biology*, *51*, 141-165.
- Li, F., Zhang, C., Tang, Z., Zhang, L., Dai, Z., Lyu, S., Li, Y., Hou, X., Bernards, M., & Wang, A. (2020). A plant RNA virus activates selective autophagy in a UPR-dependent manner to promote virus infection. *New Phytologist*, *228*(2), 622–639.
- Li, J., Huang, J., Yin, J., Wu, N., Song, J., Zhang, L., & Jiang, T. (2012). Rapid purification and characterization of γ -glutamyl-transpeptidase from shiitake mushroom (*Lentinus Edodes*). *Journal of Food Science*, *77*(6), 640-645.
- Liao, D., Pajak, A., Karcz, S. R., Patrick Chapman, B., Sharpe, A. G., Austin, R. S., Datla, R., Dhaubhadel, S., & Marsolais, F. (2012). Transcripts of sulphur metabolic genes are coordinately regulated in developing seeds of common bean lacking phaseolin and major lectins. *Journal of Experimental Botany*, *63*(17), 6283–6295.
- Liu, Z., Duan, Z., Zhang, D., Xiao, P., Zhang, T., Xu, H., Wang, C.-H., Rao, G.-W., Gan, J., Huang, Y., Yang, C.-G., & Dong, Z. (2022). Structure–Activity Relationships and Antileukemia Effects of the Tricyclic Benzoic Acid FTO Inhibitors. *Journal of Medicinal Chemistry*.
- Luna-Vital, D. A., Mojica, L., González de Mejía, E., Mendoza, S., & Loarca-Piña, G. (2015). Biological potential of protein hydrolysates and peptides from common bean (*Phaseolus vulgaris* L.): A review. *Food Research International*, *76*, 39–50.

- Martin, M. N., Cohen, J. D., & Saftner, R. A. (1995). A New 1-Aminocyclopropane-1-Carboxylic Acid-Conjugating Activity in Tomato Fruit. *Plant Physiology*, *109*(3), 917–926.
- Maruyama, A., Ishizawa, K., Takagi, T., & Esashi, Y. (1998). Cytosolic β -Cyanoalanine synthase activity attributed to cysteine synthases in cocklebur seeds. purification and characterization of cytosolic cysteine synthases. *Plant Cell Physiol*, *39* (7), 671-680.
- Matamoros, M. A., Moran, J. F., Iturbe-Ormaetxe, I., Rubio, M. C., & Becana, M. (1999). Glutathione and homoglutathione synthesis in legume root nodules. *Plant Physiol*, *121*(3), 879-888.
- McClellan, P., Gepts, P., & Kamir, J. (2004). Genomics and Genetic Diversity in Common Bean. In R. F. Wilson, H. T. Stalker & E. C. Brummer (Eds.), *Legume Crop Genomics* (pp. 60–82). Champaign, Ill: AOCS Publishing.
- Meister, A. (1995). Glutathione biosynthesis and its inhibition. In J. Abelson, M. Simon, G. Verdine (Eds.), *Methods in Enzymology* (pp. 26–30). New York, NY: Academic Press.
- Mori, M., Jeelani, G., Masuda, Y., Sakai, K., Tsukui, K., Waluyo, D., Tarwadi, Watanabe, Y., Nonaka, K., Matsumoto, A., Ōmura, S., Nozaki, T., & Shiomi, K. (2015). Identification of natural inhibitors of *Entamoeba histolytica* cysteine synthase from microbial secondary metabolites. *Frontiers in Microbiology*, *6*, 962.
- Müller, M., Voss, M., Heise, C., Schulz, T., Bünger, J., & Hallier, E. (2001). High-performance liquid chromatography/fluorescence detection of S -methylglutathione formed by glutathione- S -transferase T1 *in vitro*. *Archives of Toxicology*, *74*(12), 760–767.
- Nazir, Y., Saeed, A., Rafiq, M., Afzal, S., Ali, A., Latif, M., Zuegg, J., Hussein, W. M., Fercher, C., Barnard, R. T., Cooper, M. A., Blaskovich, M. A. T., Ashraf, Z., & Ziora, Z. M. (2020). Hydroxyl substituted benzoic acid/cinnamic acid derivatives: Tyrosinase inhibitory kinetics, anti-melanogenic activity and molecular docking studies. *Bioorganic & Medicinal Chemistry Letters*, *30*(1), 126722.
- Nelson, B. K., Cai, X., & Nebenführ, A. (2007). A multicolored set of *in vivo* organelle markers for co-localization studies in *Arabidopsis* and other plants. *The Plant Journal*, *51*(6), 1126–1136.
- O'Rourke, J. A., Iniguez, L. P., Fu, F., Bucciarelli, B., Miller, S. S., Jackson, S. A., McClellan, P. E., Li, J., Dai, X., Zhao, P. X., Hernandez, G., & Vance, C. P. (2014). An RNA-Seq based gene expression atlas of the common bean. *BMC Genomics*, *15*(1), 866.
- Okada, M., & Kimura, Y. (2022). Characterization of glutamate-cysteine ligase and glutathione synthetase from the δ -proteobacterium *Myxococcus xanthus*. *Proteins: Structure, Function, and Bioinformatics*, *90*(8), 1547–1560.
- Osborn, T. C., Hartweck, L. M., Harmsen, R. H., Vogelzang, R. D., Kmiecik, K. A., & Bliss, F. A. (2003). Registration of *phaseolus vulgaris* genetic stocks with altered seed protein compositions. *crop science*, *43*(4), 1570–1571.
- Rathbun, W. B. (1967). γ -Glutamyl-cysteine synthetase from bovine lens. *Archives of Biochemistry and Biophysics*, *122*(1), 73–84.

- Rébeillé, F., Jabrin, S., Bligny, R., Loizeau, K., Gambonnet, B., van Wilder, V., Douce, R., & Ravanel, S. (2006). Methionine catabolism in *Arabidopsis* cells is initiated by a γ -cleavage process and leads to S-methylcysteine and isoleucine syntheses. *Proceedings of the National Academy of Sciences*, *103*(42), 15687–15692.
- Saboori-Robat, E., Joshi, J., Pajak, A., Renaud, J., Marsolais, F., Sol, M., Maccelli, C., Joshi, J., Marsolais, F., Joshi, J., & Mohsenpour, M. (2019). Common bean (*Phaseolus vulgaris* L.) accumulates most S-methylcysteine as its glutamyl dipeptide. *Plants*, *8*(5), 126.
- Scheller, H. v., Huang, B., Hatch, E., & Goldsbrough, P. B. (1987). Phytochelatin synthesis and glutathione levels in response to heavy metals in tomato cells. *Plant Physiology*, *85*(4), 1031–1035.
- Servillo, L., Giovane, A., Balestrieri, M. L., Ferrari, G., Cautela, D., & Castaldo, D. (2012). Occurrence of pipercolic acid and pipercolic acid betaine (homostachydrine) in citrus genus plants. *Journal of Agricultural and Food Chemistry*, *60*(1), 315–321.
- Sgarbieri, V. C., & Whitaker, J. R. (1982). Physical, chemical, and nutritional properties of common bean (*Phaseolus*) protein. In C. O. Chichester, E. M. Mrak, & G. F. Stewart (Eds.), *Advances in food research* (pp. 93-151). New York, NY: Academic Press.
- Shimabukuro, R. H., Swanson, H. R., & Walsh, W. C. (1970). Glutathione conjugation: atrazine detoxication mechanism in corn. *Plant Physiology*, *46*(1), 103–107.
- Sørensen, H., & Mortensen, K. (2005). Soluble expression of recombinant proteins in the cytoplasm of *Escherichia coli*. *Microbial Cell Factories*, *4*(1), 1.
- Sparkes, I. A., Runions, J., Kearns, A., & Hawes, C. (2006). Rapid, transient expression of fluorescent fusion proteins in tobacco plants and generation of stably transformed plants. *Nature Protocols*, *1*(4), 2019–2025.
- Sullivan, J. G. (1981). Recurrent Selection for Increased Seed Yield and Percentage Seed Protein in the Common Bean (*Phaseolus Vulgaris* L.): Using a Selection Index; and Isolation and Analysis of Major Genes Controlling Phaseolin (Doctoral dissertation, The University of Wisconsin-Madison, Madison, United State). Retrieved from https://books.google.ca/books/about/Recurrent_Selection_for_Increased_Seed_Y.html?id=RHzUAAAAMAAJ&redir_esc=y.
- Suzuki, H., & Kumagai, H. (2002). Autocatalytic processing of γ -glutamyltranspeptidase. *Journal of Biological Chemistry*, *277*(45), 43536–43543.
- Takahashi, H. (2010). Regulation of sulfate transport and assimilation in plants. *International Review of Cell and Molecular Biology*, *281*(C), 129–159.
- Takahashi, H., Kopriva, S., Giordano, M., Saito, K., & Hell, R. (2011). Sulphur assimilation in photosynthetic organisms: Molecular functions and regulations of transporters and assimilatory enzymes. *Annual Review of Plant Biology*, *62*, 157–184.
- Tang, Z., Bernards, M. A., & Wang, A. (2022). Simultaneous determination and subcellular localization of protein–protein interactions in plant cells using bimolecular fluorescence

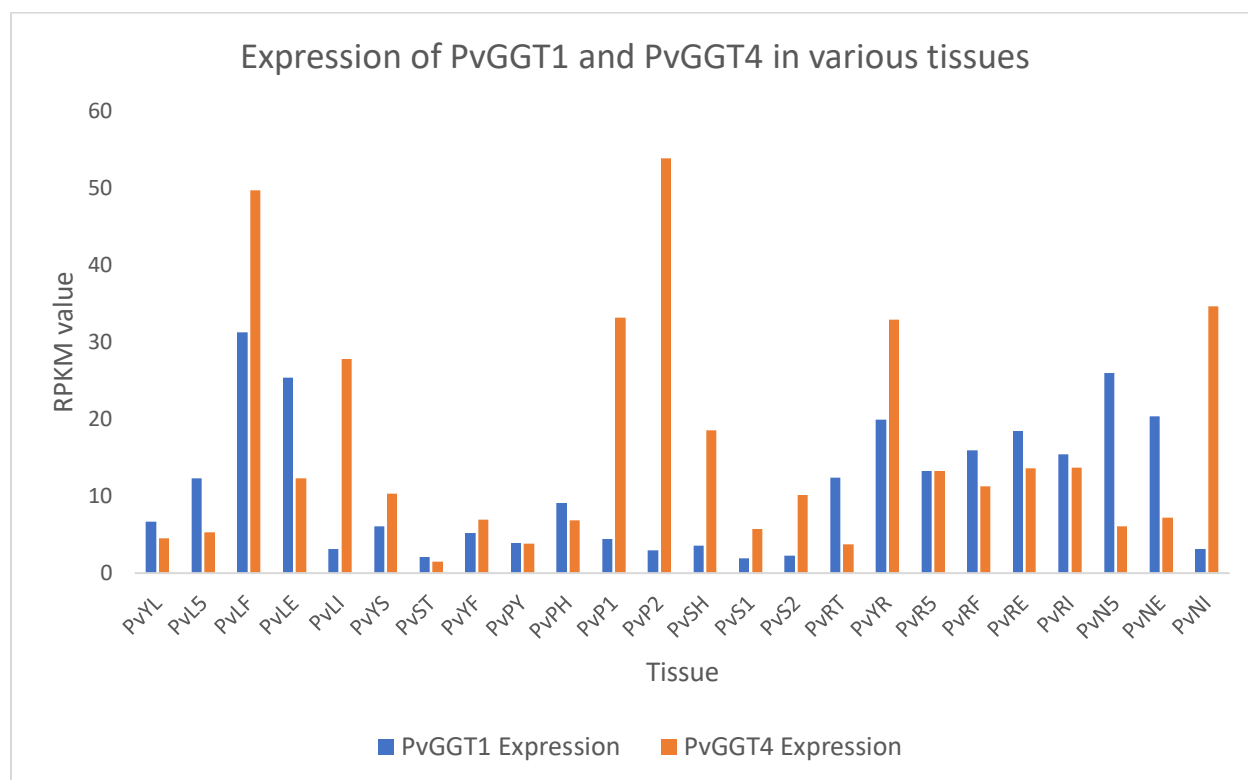
- complementation assay. In J. M. Walker (Eds.), *Methods in Molecular Biology* (pp. 75–85). Totowa, NJ: Humana Press.
- Tate, S. S., & Meister, A. (1981). γ -Glutamyl transpeptidase: catalytic, structural and functional aspects. *Molecular and Cellular Biochemistry*, *39*(1), 357–368.
- Taylor, M., Chapman, R., Beyaert, R., Hernández-Sebastià, C., & Marsolais, F. (2008). Seed storage protein deficiency improves sulphur amino acid content in common bean (*Phaseolus vulgaris* L.): Redirection of sulphur from γ -glutamyl-S-methyl-cysteine. *Journal of Agricultural and Food Chemistry*, *56*(14), 5647–5654.
- Thompson, J. F., & Gering, R. K. (1966). Biosynthesis of S-methylcysteine in radish leaves. *Plant Physiology*, *41*(8), 1301–1307.
- Thompson, J. F., Turner, D. H., & Gering, R. K. (1964). γ -Glutamyl transpeptidase in plants. *Phytochemistry*, *3*(1), 33–46.
- Todd, M. J., & Gomez, J. (2001). Enzyme kinetics determined using calorimetry: a general assay for enzyme activity? *Analytical Biochemistry*, *296*(2), 179–187.
- Walbot, V., Clutter, M., & Sussex, I. (1972). Reproductive development and Embryogeny in *Phaseolus*. *Phytomorphology* *22*, 59-68.
- Wei, T., Huang, T.-S., McNeil, J., Laliberté, J.-F., Hong, J., Nelson, R. S., & Wang, A. (2010). Sequential recruitment of the endoplasmic reticulum and chloroplasts for plant potyvirus replication. *Journal of Virology*, *84*(2), 799–809.
- Widhalm, J. R., & Dudareva, N. (2015). A familiar ring to it: biosynthesis of plant benzoic acids. *Molecular Plant*, *8*(1), 83–97.
- Yoshimoto, N., Yabe, A., Sugino, Y., Murakami, S., Sai-ngam, N., Sumi, S., Tsuneyoshi, T., & Saito, K. (2015). Garlic γ -glutamyl transpeptidases that catalyze deglutamylation of biosynthetic intermediate of alliin. *Frontiers in Plant Science*, *5*, 758.

Appendices



Appendix A: Expression profile of candidate genes in various plant tissues

Description of plant tissues are as follows: PvYL - Fully expanded 2nd trifoliolate leaf tissue; PvL5 - Leaf tissue collected 5 days after plants were inoculated with effective rhizobium; PvLF - Leaf tissue collected 21 days after fertilized plants; PvLE - Leaf tissue collected 21 days after plants were inoculated with effective rhizobium; PvLI - Leaf tissue collected 21 days after plants were inoculated with ineffective rhizobium; PvYS - All stem internodes above the cotyledon collected at the 2nd trifoliolate stage; PvST - Shoot tip, including the apical meristem, collected at the 2nd trifoliolate stage; PvFY - Young flowers, collected prior to floral emergence; PvPY - Young pods, collected 1 to 4 days after floral senescence; PvPH - Pods approximately 9 cm long, (pod only); PvP1 - Pods between 10 and 11 cm long (pod only); PvP2 - Pods between 12 and 13 cm long (pod only); PvSH - Heart stage seeds, approximately 7 mg; PvS1 – seeds approximately 50 mg; PvS2 – seeds between 140 and 150 mg; PvRT - Root tips collected from fertilized plants at 2nd trifoliolate stage of development; PvYR - Whole roots, including root tips, collected at the 2nd trifoliolate stage of development; PvR5 - Whole roots separated from 5-day-old pre-fixing nodules; PvRF - Whole roots from fertilized plants collected 21 days after inoculation; PvRE - Whole roots separated from fix+ nodules collected 21 days after inoculation; PvRI - Whole roots separated from fix- nodules collected 21 days after inoculation; PvN5 - Pre-fixing (effective) nodules collected 5 days after inoculation; PvNE - Effectively fixing nodules collected 21 days after inoculation; PvNI - Ineffectively fixing nodules collected 21 days after inoculation (O'Rourke et al., 2014).



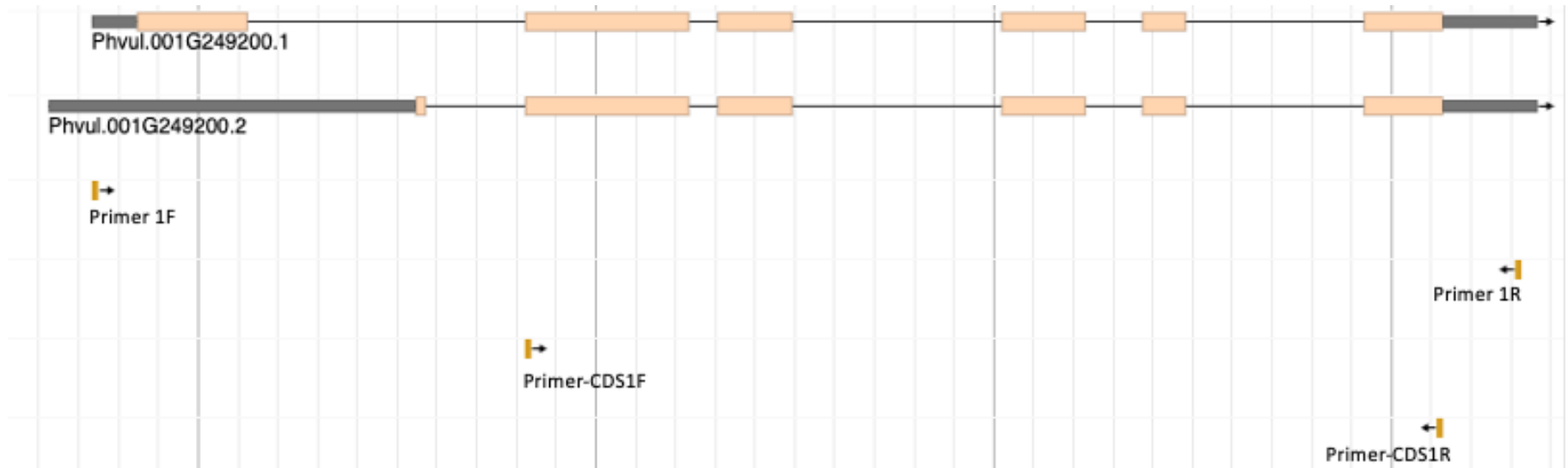
Appendix B: Expression profile of PvGGT1 and PvGGT4 in various plant tissues.

Description of plant tissues are mentioned in appendix A legend (O'Rourke et al., 2014).

EcGGT	-MRRSFLKTI GLGVIALFLGLLNPLSAASY PPI-----KNTKVG LALSSHP	45
HpGGT	MIKPTFLRRVAIAA--LLSGSC--FSAAAAPPAPVSYGVEEDVFHPVRAKQGMVASVDA	56
PvGGT1	-----	0
PvGGT4	-----MRRSSKGDIAESDVG VVATDDA	21
EcGGT	LASEIGQKVLEEGGNAIDAAVAIGFALAVVHPAAGNIGGGGFAVIHLAN-GENVALDFRE	104
HpGGT	TATQVGV DILKEGGNAVDAAVAVGYALAVTHPQAGNLGGGGFMLIRSKN-GNTTAIDFRE	115
PvGGT1	-----MVC	3
PvGGT4	RCSAIGVSVIKQGGHAVDAAVAAALCIGVVLSVSSGIGGGGFMVVRSSSTSQTQAFDMRE	81
	:	
EcGGT	KAPLKATKNMFLDKQGNVVPKLS EDGYLAAGVPGTVAGMEAMLKKG YTKKLSQLIDPAIK	164
HpGGT	MAPAKATRDMFLDDQGNPDSKKS L TSHLASGTPGT VAGFSLALDKYGT MPLNKVVQP AFK	175
PvGGT1	AKDAPMFQDMYGGN-----TTLKAQGGLSVAVPGELAGLHEAWKQY GKL PWKRLVNP AEN	58
PvGGT4	TAPAAASQNMYEKN-----LKDKSLGVLSMGVPGELAGLHAAWLKYGR LPWKTLFQPAIE	136
	::*: . . . *: .** :** : ** . : : ** :	
EcGGT	LAENGYAISQRQAETLKEARERFLKYSSSKKYFFKKGHLDYQEGDLFVQKDLAKTLNQIK	224
HpGGT	LARDGFIVNDALADDLKYGSEVLPNHENSKAIFWKEGEPLKKGDTLVQANLAKSLEMIA	235
PvGGT1	LARRGFKISAYLHMOMKSTESDILQDKGLRS-ILAPNGKLLNIGDTCYNKKLADTLRAIS	117
PvGGT4	LAEKGFVVPALGNFIVTDAEKILDDPGLRK-LYAPKGALLKEGDVCKNAELGLTLEIVA	195
	** . * : : . : . . * . : : : * : * : . * . : * . :	
EcGGT	TLGAKGFYQGGVAELIEKDMKNGGIITKEDLASYNVWKRPVVGSYRKYKII SMSPPSS	284
HpGGT	ENGPDEFYKGTIAEQIAQEMQKNGGLITKEDLAAYKAVERTPI S G DY RGYQVYSMP PPS	295
PvGGT1	VFGPKAFYDGLIGHNLVKDVQNA GGILTTKDLKNYTVNQKKPLSTNVLGLNLLAMP PPSG	177
PvGGT4	EQGPQAFYNGSIAEKLVKDVKEAGGILTMEDLRNYKLEIADAMTLNVMGYTIYGM PPS	255
	* . ** . * : : : : : : ** : * : * : . * : . * * * * .	
EcGGT	GGTHLIQILNV MENADLSALGYGASKNIHIAAEAMRQAYADR SVYMGDADFVSVP---VD	341
HpGGT	GGIHIVQILNILENFDMKKYGFGSADAMQIMAEAEKYAYADRSEYLGDPDFVKVP---WQ	352
PvGGT1	GP-PMILLNILDQYKLP SGLS-GALGIHREIEALKHVF A VR-MNLGDPDFVN-ITEVVS	233
PvGGT4	GTLALS LVLNILD SYGDPDAAR-GNLGVHRLIEALKFMFAIR-MNLGDPNFVENIDDTIS	313
	* : : ** : : . . : : ** : : * * : ** : ** . .	
EcGGT	KLINKAYAKKIFD TIQPD TVTPSSQIKPGMGQLHEGSNTTHYSVADR WGN AVSVTYTINA	401
HpGGT	ALTNKAYAKSIADQIDINKAKPSSEIRPGK L APYESNQ TTHYSVVDKDGNAVAVTYTLNT	412
PvGGT1	DMLSRRAFATVLKNDINDNKTFSP THY-GGKWNQIHDHGTSHLCVIDLERN AISMTT TVNA	292
PvGGT4	KMLSPSFAKEIQQKILDNTTFFPEY Y-MNRWSQLRDHGTSHMCIVDADRNAVSLTSTVNY	372
	: . : * . : : * : : . . * : * : * : * : * : * : * : *	
EcGGT	SYGSAASIDGAGFLLNEMDDFSIKPGNPNLYGLVGGDANAIEANKRPLSSMSPTIVLKN	461
HpGGT	TFGTGIVAGESGILLNNQMDDFS AKPGV PNVYGLVGGDANAVGPNKRPLSSMSPTIVVKD	472
PvGGT1	YFGSKILSPSTGIVLNNEMDDFSI PRNVS-KDVPPPAPS NFIMPGRPLSSMSPTIALKD	351
PvGGT4	HFGAGFRSVSTGILVNNEMDDFSAPTEIT-PDKLPPAPANFIEPNKRPLSSMTPLIITKD	431
	::* : : ** : * * * * * . : * : . * * * * * : * * *	
EcGGT	NKVFLVVGSPGCSRIITTVLQVISNVIDYNNMISEAVSAPRFHMQLPDELRIEKFGM--	519
HpGGT	GKTWLVGSPGCSRIITTVLQMVVNSIDYGLNVAEATNAPRFHHQWLPDEL RVEKGF S--	530
PvGGT1	GKLKAVVGASGGAFFIIGGTSEVLLNHFGKGLDPFSSVTAPRVYHQLIPNVVNYENWTTVT	411
PvGGT4	DELVGVLGSGCMNIAPAVIQIFINHFILGMKPLDAVMSPRIYHKLIPNVVRYENLTALN	491
	. : * * . * * . . : . * : . . . : ** . : : * : : . * :	
EcGGT	-----PADVKDNLTKMGYQIVTKPVMGDVNAIQVLP-----KTKGSVF	557
HpGGT	-----PDT-LKLEAKGQKVALKEAMGSTQSIMVGP-----DGEL	564
PvGGT1	GDHFELGADIRKVLRSKGHVLSLAGGTICQFIVVENS VSS-----RKTKV TGIERL	463
PvGGT4	GDHIQFSKERRIFLEERGHQLSECEALAVTQLVVQNLKTPVKMNRKIGKNINLQSKHGTL	551
	* * : : : :	

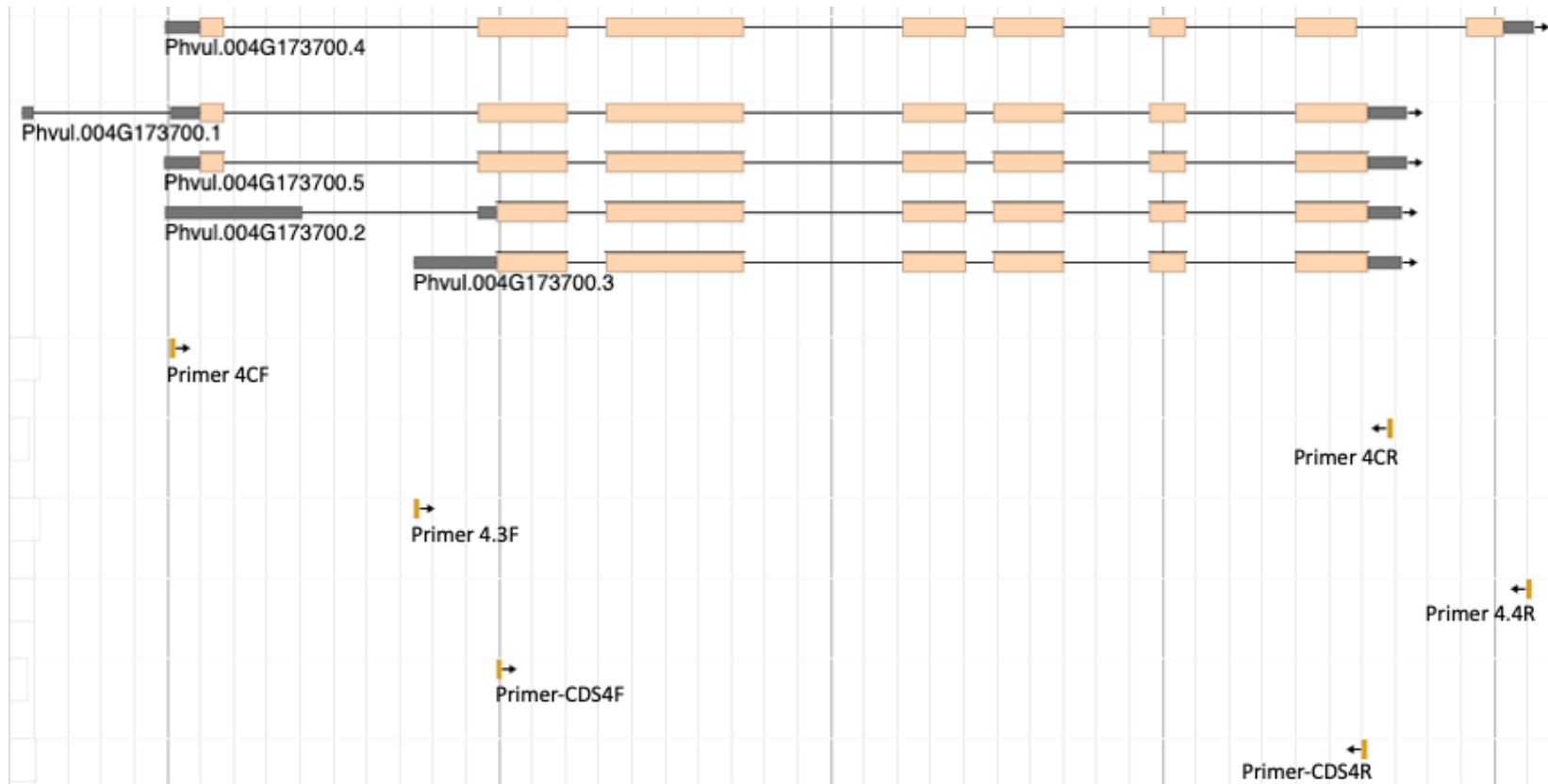
Appendix C: Multiple sequence alignment of *EcGGT*, *HpGGT* and *PvGGT1*, *PvGGT4*.

The putative internal cleavage sites for *PvGGT1* and *PvGGT4* are highlighted in yellow, which are Thr²⁷¹ and Thr³⁵², respectively. Other highly conserved and potentially reactive amino acids are highlighted in blue and green (Castellano et al., 2010).



Appendix D: PvGGT1 primers for RT-PCR experiment align with transcripts of PvGGT1.

PvGGT1 transcripts include untranslated region (UTR, in grey) and coding sequence (CDS, in caramel). Forward (Primer 1F) and reverse (Primer 1R) primers were designed for both transcripts in the RT-PCR experiment. Forward and reverse primers designed from coding sequence of PvGGT1 are Primer-CDS1F and Primer-CDS1R, respectively (www.phytozome.net).



Appendix E: PvGGT4 primers for RT-PCR experiment align with transcripts of PvGGT4.

PvGGT4 transcripts include untranslated region (UTR, in grey) and coding sequence (CDS, in caramel). There are common forward and reverse primers for all transcripts, which are Primer 4CF and Primer 4CR, respectively. Primer 4.3F is the specific forward primer for transcript PvGGT4.3; and Primer 4.4R is the specific reverse primer for transcript PvGGT4.4. Forward and reverse primers designed from coding sequence of PvGGT4 are Primer-CDS4F and Primer-CDS4R, respectively (www.phytozome.net).

Curriculum Vitae

Name: Zixuan Lu

Post-secondary Education and Degrees: Hefei University of Technology
Hefei, Anhui, China
2015-2017 BSc.

University of Waterloo
Waterloo, Ontario, Canada
2017-2020 BSc.

The University of Western Ontario
London, Ontario, Canada
2020-2022 MSc candidate.

Honours and Awards: Dean's Honours List
University of Waterloo
2017-2020

Western Graduate Research Scholarship
Western University
2020-2022

Related Work Experience Research Affiliate
Agriculture and Agri-Food Canada
2020-2022

Teaching Assistant
The University of Western Ontario
2020-2021

Research Assistant
University of Waterloo
2019-2020

Publications:

Braniff, N., Pearce, T., **Lu, Z.**, Astwood, M., Forrest, W., Receno, C., Ingalls, B. (2022). NLoed: A Python Package for Nonlinear Optimal Experimental Design in Systems Biology. *Biotech Week* (p. 664–). NewsRX LLC.